

8-1-1989

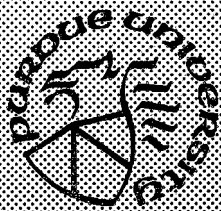
The DQ Analysis of a Variable Reluctance Stepper Motor

David J. Kish
Purdue University

Follow this and additional works at: <https://docs.lib.purdue.edu/ecetr>

Kish, David J., "The DQ Analysis of a Variable Reluctance Stepper Motor" (1989). *Department of Electrical and Computer Engineering Technical Reports*. Paper 669.
<https://docs.lib.purdue.edu/ecetr/669>

This document has been made available through Purdue e-Pubs, a service of the Purdue University Libraries. Please contact epubs@purdue.edu for additional information.



The DQ Analysis of a Variable Reluctance Stepper Motor

D. J. Kish

**TR-EE 89-38
August, 1989**

**School of Electrical Engineering
Purdue University
West Lafayette, Indiana 47907**

this is dedicated
to my parents

ACKNOWLEDGMENTS

I would like to thank my family and friends for their support and encouragement. I am indebted to Professor Krause not only for his guidance throughout this year, but also for his assistance while I was applying for admission to graduate school. A special thanks to Professor Ong and Professor Wasynczuk for agreeing to serve on my thesis committee. Finally, I wish to express my gratitude to Professor Heydt and to the sponsors of the Purdue Electric Power Center for the financial support which enabled me to return to school and obtain this degree.

TABLE OF CONTENTS

	Page
LIST OF TABLES	vi
LIST OF FIGURES.....	vii
ABSTRACT.....	ix
CHAPTER 1 - INTRODUCTION.....	1
CHAPTER 2 - DESCRIPTION OF A VARIABLE RELUCTANCE STEPPER MOTOR.....	3
2.1 Introduction.....	3
2.2 Motor Operation	3
2.3 Bipolar Drives	7
2.4 Electrical Model for the Motor.....	7
2.5 Electrical Torque	9
2.6 Shaft Dynamics	10
2.7 State Variable Model.....	10
CHAPTER 3 - THE DQ TRANSFORMATION APPLIED TO A VARIABLE RELUCTANCE STEPPER MOTOR.....	12
3.1 Motivation for DQ Analysis.....	12
3.2 DQ Analysis	12
3.3 Effect of the DQ Transformation on Flux Linkages.....	14
3.4 Transformed Voltage Equations.....	15
CHAPTER 4 - COMPARISON OF RESULTS FOR DETAILED AND AVERAGE DQ SIMULATION	17
4.1 Introduction	17
4.2 Numerical Integration	17
4.3 Device Parameters and Mode of Operation	18

4.4	Currents at Constant Speed	18
4.5	Machine Torques	22
CHAPTER 5 - APPLICATIONS OF THE AVERAGE MODEL.....		25
5.1	Introduction	25
5.2	Impact of a Change in Motor Resistance on Average Torque.....	25
5.3	Torque Delta Curves	30
5.4	Dynamic Simulation - Steady State.....	30
5.5	Dynamic Simulation - Step Change in Load Torque	40
5.6	Explanation of Model Differences	40
CHAPTER 6 - SUMMARY AND CONCLUSIONS		50
LIST OF REFERENCES		51

LIST OF TABLES

Table	Page
4.1 Motor parameters	19
4.2 Comparison of machine currents.....	19
4.3 Comparison of machine torques.....	19
5.1 Comparison of state models.....	25
5.2 Rotor angle from simulations compared with rotor angle from torque vs. δ curves.....	39

LIST OF FIGURES

Figure	Page
2.1 Cutaway view of a variable-reluctance stepper motor	4
2.2 Minimum reluctance rotor position.....	6
2.3 Maximum reluctance rotor position	6
2.4 Phase A of bipolar voltage waveform	8
4.1 Machine currents (steady state, detailed inductance matrix)	20
4.2 Machine currents (steady state, averaged inductance matrix).....	21
4.3 Machine torque from the detailed model.....	23
4.4 Machine torque from the averaged model	24
5.1 Machine currents (detailed model, $R = 200 \Omega$)	26
5.2 Machine currents (averaged model, $R = 200 \Omega$).....	27
5.3 Machine torque from the detailed model ($R = 200 \Omega$).....	28
5.4 Machine torque from the averaged model ($R = 200 \Omega$).....	29
5.5 Machine torque vs. δ (detailed model).....	31
5.6 Machine torque vs. δ (averaged model)	32
5.7 Machine currents and rotor angle vs. time (detailed model, damping only).....	33

5.8 Angular velocity and machine torque vs. time (detailed model, damping only).....	34
5.9 Machine currents and rotor angle vs. time (detailed model, expanded time scale, damping only)	35
5.10 Angular velocity and machine torque vs. time (detailed model, expanded time scale, damping only)	36
5.11 Machine currents and rotor angle vs. time (averaged model, damping only)	37
5.12 Angular velocity and machine torque vs. time (averaged model, damping only)	38
5.13 Machine currents and rotor angle vs. time (detailed model, load applied).....	41
5.14 Angular velocity and machine torque vs. time (detailed model, load applied).....	42
5.15 Machine currents and rotor angle vs. time (averaged model, load applied)	43
5.16 Angular velocity and machine torque vs. time (averaged model, load applied)	44
5.17 Machine currents and rotor angle vs. time (detailed model, load removed).....	45
5.18 Angular velocity and machine torque vs. time (detailed model, load removed).....	46
5.19 Machine currents and rotor angle vs. time (averaged model, load removed)	47
5.20 Angular velocity and machine torque vs. time (averaged model, load removed)	48

ABSTRACT

David J. Kish. M.S.E.E., Purdue University. August 1989. The DQ Analysis of a Variable Reluctance Stepper Motor. Major Professor: Paul Krause

Variable reluctance stepper motors are commonly used in applications where incremental motion is desired. Recently, these motors have been used in situations which call for a large stepping rate; so large in fact, that the motor turns continuously. Although the equations which describe the stepper motor in this mode are decoupled, they are not time invariant. In order to eliminate the time varying terms, Park's transformation is applied to the motor equations. It is found that this transformation does not render the system equations time invariant, so an averaging technique is employed which does provide the desired time invariance. The averaged model is evaluated by comparing its dynamic response with that of a detailed simulation of the motor in a variety of operating modes. It is found that the averaged model does not adequately represent the motor dynamics under most operating conditions.

CHAPTER 1 INTRODUCTION

This thesis deals with stepper motors. In general, there are two types of stepper motors, the permanent magnet motor and the variable reluctance motor. The latter type is the subject of this thesis.

The name "stepper motor" is appropriate since there are a discrete number of locations at which the rotor will come to rest when the windings of the motor are supplied by a dc source. When the dc source is applied to the different windings successively, the motor steps from position to position. Stepper motors have often been used in conjunction with digital control systems. If each discrete rotor position is represented by a binary number, interfacing the digital output of the controller with the motor is not difficult.

Positioning systems which use stepper motors can be quite precise, in fact, these motors have been used to position radar antennas to within 30 seconds of arc of a desired location. Another application which takes advantage of both the positioning capabilities of the motor as well as its inherent digital system compatibility is a computer disc drive. Here, the disc head is accurately moved from sector to sector in order to read the information stored on the disc.

Stepper motors have certain practical features which make them particularly attractive to industry in terms of both manufacturing and applications. First, stepper motors are relatively easy to assemble. Because these motors are designed with "teeth" on the stator, it is not difficult to wind the stator. From an economic standpoint, step motor drive systems can be designed which use only one power semiconductor per machine phase. Also, control systems can be quite simple, as the motor's positioning capabilities do not require a closed-loop controller. Like induction motors, stepper motors do not have slip rings or brushes which are features of dc and synchronous machines. For this reason, stepper motors can be used in hostile, possibly explosive environments where the use of a motor with brushes is not advisable.

For the most part, these motors have been used in the positioning applications for which they are particularly suited. Recently, stepper motors have been used in both open and closed loop systems for continuous speed operation. In this mode, stepper motors can produce more power per given volume than can an induction motor with about the same power factor. Rotor heating is reduced in the stepper motor since the machine is not designed to have rotor currents flowing.

The familiar torque speed curve of an induction machine is quite useful in the design of systems using this motor. This curve can be predicted analytically [1],[2]; however, in the case of the stepper motor, such curves are often obtained experimentally. Transfer function formulations are helpful in system design; in fact, the transfer function of a dc motor is often used as a practical example of a transfer function in control systems texts [3]. A corresponding simple transfer function for the stepper motor does not exist. When stepper motors are operated in the continuous mode (also referred to as high frequency operation), a velocity oscillation is superimposed on the synchronous speed of the motor. These oscillations can reduce the torque produced by the motor and cause a loss of synchronism. This loss of synchronism is referred to as parametric instability.

A means of analysis which would provide an expression for a torque speed curve while also showing the parametric instability of the motor would be useful. Perhaps equally useful is a technique by which the machine equations can be couched to permit linearization and a transfer function formulation. Reference frame theory has been used for such purposes with both induction and synchronous machines, and it will be applied in the analysis which follows. This thesis is divided into five additional chapters. Chapter 2 discusses the operation of a variable reluctance stepper motor and presents the basic equations which are used in its analysis. In Chapter 3, the equations which were derived in Chapter 2 are transformed to the dq reference frame, and certain simplifying assumptions are made. Chapter 4 and Chapter 5 present simulation results for the complete and simplified models of the motor. Finally in Chapter 6, simulation results are summarized, and recommendations on the use of the simplified model are made.

CHAPTER 2

DESCRIPTION OF A VARIABLE RELUCTANCE STEPPER MOTOR

2.1 Introduction

The machine to be analyzed is a two pole, three stack, variable reluctance stepper motor. This particular device has two rotor teeth and two stator teeth. Fig - 2.1 shows a cross section of a three stack variable reluctance machine. While this figure shows the physical construction of a variable reluctance stepper motor, it is more complicated than the one under analysis due to a greater number of stator and rotor teeth. In this chapter, a general explanation of motor operation will be provided, and an expression for step length is obtained. Next, an electrical model of the motor will be developed by examining one phase (stack) of the motor. The mechanical equations which describe the motor will be explained, and a state variable representation of the motor will be obtained.

2.2 Motor Operation

As its name implies, the operation of this motor depends upon the variable reluctance path the device provides to the flux developed by current in each phase winding. In a coupled electro-mechanical system, a force is developed in order to minimize the reluctance path seen by the flux linkages. A familiar application of this principle is an ordinary electromagnet. When current flows in the magnet windings, a force is developed which "picks up" a piece of metal. Originally, there was a high reluctance air-gap between the electromagnet and the metal. When the metal and magnet are touching, there is very little air gap, rather, a low reluctance path through the metal exists for the flux linkages. The force generated by the magnet acted to minimize the reluctance in the system.

Examination of the geometry of the stepper motor shows there is a minimum and maximum reluctance position. Fig - 2.2 shows the minimum

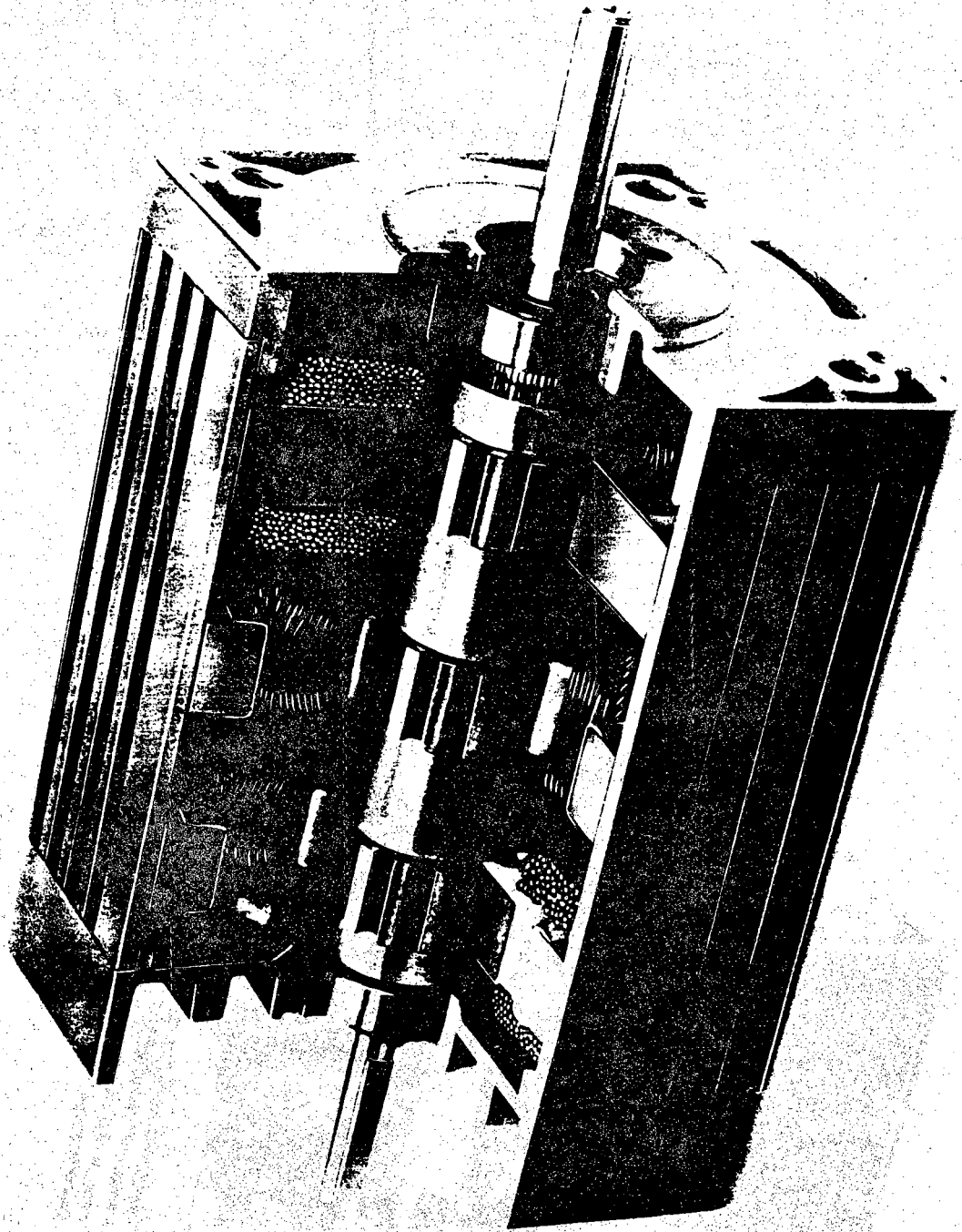


Figure 2.1 Cutaway view of a variable-reluctance stepper motor.

reluctance rotor position for the motor, while the maximum reluctance position is shown in Fig - 2.3. When the windings are energized, the flux must cross a large air gap in the maximum reluctance position. In the minimum reluctance position, the flux is for the most part contained within the stator back iron and the rotor. Since a force (torque) is developed to minimize the reluctance path, it is expected that a torque to move the rotor from the position shown in Fig - 2.3 to that of Fig - 2.2 exists. If the rotor is positioned in the minimum reluctance position, such a torque should not exist. This is what occurs in practice.

Assume the windings in stack A have a current flowing in them. The rotor will move to the minimum reluctance position and remain there. Now the minimum reluctance position for stack A is not the minimum reluctance position for stack B or stack C. If the current flowing in stack A is shut off, and at the same time, a current is made to flow in the windings of stack B, the rotor will move to the minimum reluctance position of stack B. The rotor has just "stepped" from one minimum reluctance position to another.

An expression for the distance between these minimum reluctance positions is desired. The tooth pitch (TP), i.e., the angular distance between two rotor teeth, is defined as

$$TP = \frac{2\pi}{RT}, \quad (2.2-1)$$

where RT represents the number of rotor teeth. If each stack is excited in turn, e.g., as, bs, cs, as the rotor will move one tooth pitch. The step length (SL) then is given by

$$SL = \frac{2\pi}{RT N}. \quad (2.2-2)$$

The symbol N in EQ (2.2-2) represents the number of stacks in the machine.

So far, step operation has been discussed for a no-load condition on the machine. A brief explanation of motor operation with a load torque follows. If a mechanical load is attached to the rotor while a set of windings is energized, the motor will develop a torque to try to move the rotor to the minimum reluctance position. The load will oppose this motion, and the rotor will come to rest at a position δ , where

$$T_e = T_l. \quad (2.2-3)$$

When the next winding in the excitation sequence is energized, the rotor will move to a position displaced from the new minimum reluctance position by

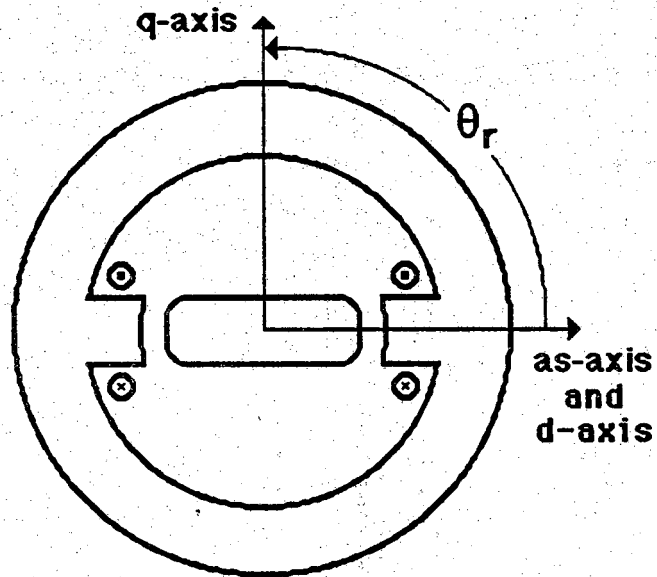


Figure 2.2 Minimum reluctance rotor position.

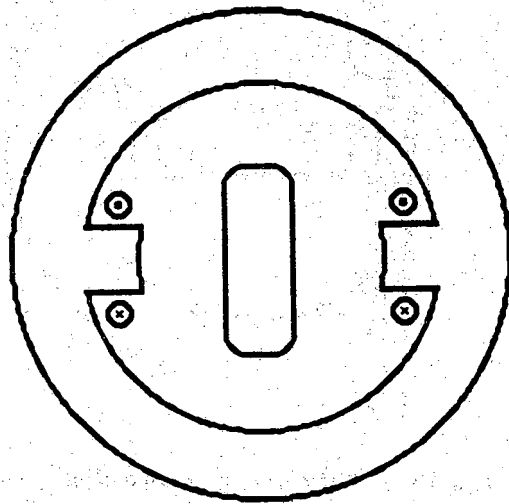


Figure 2.3 Maximum reluctance rotor position.

the same angle δ . Of course, if the load torque exceeds the electrical torque, the step motion will not occur. Instead, the rotor will rotate in the direction specified by the load torque.

2.3 Bipolar Drives

The motor will be driven by a bipolar, square wave voltage. Fig - 2.4 shows the voltage applied to phase A of the motor; The first term in the Fourier Series for this voltage waveform is also shown in Fig - 2.4; this term will be used to model the voltage applied to motor throughout the work which follows. Additional explanation of motor operation with such a voltage waveform is required before proceeding. In the previous section, it was established that the rotor will move to position itself in a minimum reluctance configuration. This position *does not* depend upon the polarity of the applied voltage. There are two implications which result from this property. First, there will be two phase A minimum reluctance positions in each period of the phase A voltage. Secondly, the motor will operate in the so-called reverse double speed mode, i.e., the rotor will turn at twice the speed it would with unipolar excitation and will rotate in a direction opposite that which would be expected if the voltage phase sequencing were considered alone.

2.4 Electrical Model for the Motor

The electrical model of the variable reluctance stepper motor will be derived by examining one stack of the machine. Once the model for one stack is obtained, the equations for the remaining stacks are obtained by a simple change of variables.

The voltage equation for a single stack of the motor is

$$v = r i + \frac{d}{dt} \lambda \quad (2.4-1)$$

where

$$\lambda = L i. \quad (2.4-2)$$

An expression for the inductance, L , in EQ (2.4-2) is needed in order to continue our work. It is known that inductance is inversely proportional to reluctance; also, from the previous discussion, the reluctance varies between a maximum and minimum value. In fact, from examination of Fig - 2.2 and Fig

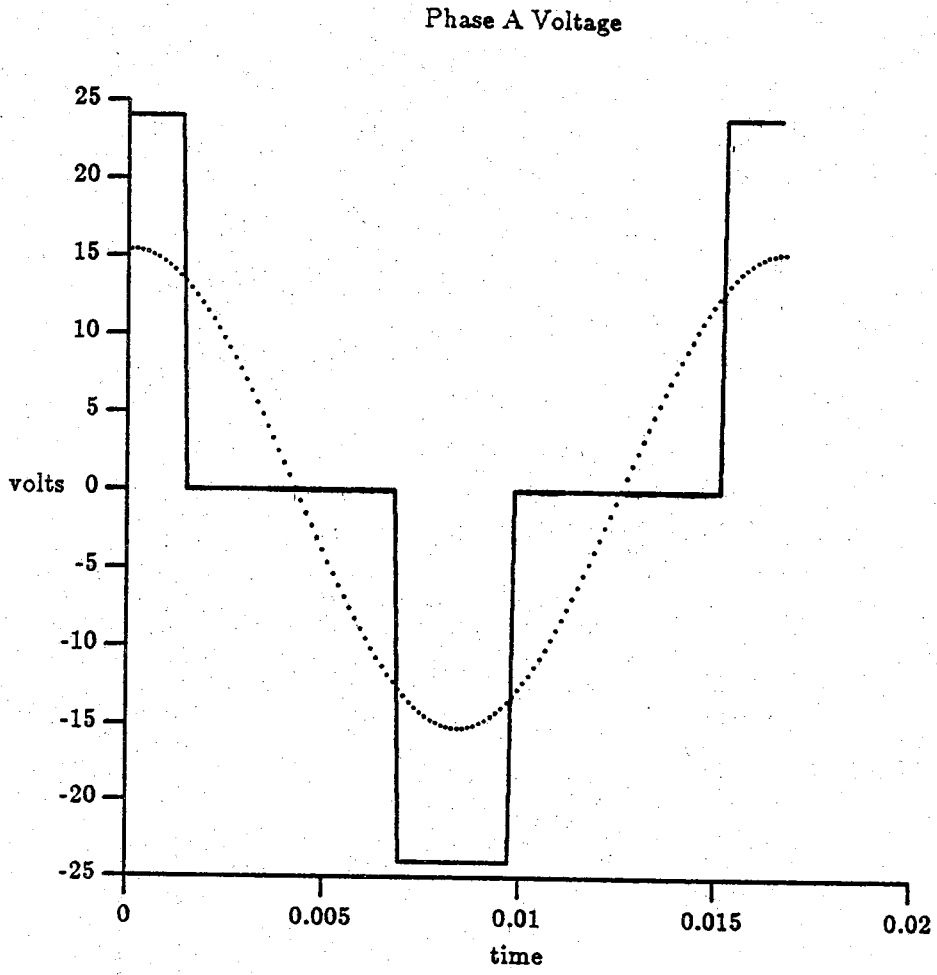


Figure 2.4 Phase A of bipolar voltage waveform.

- 2.3, it is clear that there are two maximums and two minimums of reluctance in every rotation of the rotor. Therefore, the machine's inductance will be modeled as

$$L = A - B\cos(2\theta_r), \quad (2.4-3)$$

where θ_r is defined in Fig - 2.2. Substituting EQ (2.4-2) and EQ (2.4-3) into EQ(2.4-1), the voltage equation is found to be

$$v = r i + (A - B\cos(2\theta_r)) \frac{d}{dt} i + \omega_r (2B\sin(2\theta_r)) i \quad (2.4-4)$$

where

$$\omega_r = \frac{d}{dt} \theta_r. \quad (2.4-5)$$

For an n-phase machine, the axis of each phase is displaced from the previous axis by $\frac{2\pi}{n}$. Therefore, the time varying inductance of the ith stack is

$$L = A - B\cos(2(\theta_r - \frac{i\pi}{n})). \quad (2.4-6)$$

Replacing the "L" terms in EQ (2.4-1) and EQ (2.4-2) with EQ (2.4-6), a general voltage equation for each phase is obtained. Each voltage equation is combined and written as the single matrix equation

$$\begin{bmatrix} v_a \\ v_b \\ v_c \end{bmatrix} = \begin{bmatrix} r & 0 & 0 \\ 0 & r & 0 \\ 0 & 0 & r \end{bmatrix} \begin{bmatrix} i_a \\ i_b \\ i_c \end{bmatrix} + 2B\omega_r \begin{bmatrix} \sin(2\theta_r) & 0 & 0 \\ 0 & \sin(2(\theta_r - \frac{2\pi}{3})) & 0 \\ 0 & 0 & \sin(2(\theta_r + \frac{2\pi}{3})) \end{bmatrix} \begin{bmatrix} i_a \\ i_b \\ i_c \end{bmatrix} \\ + \begin{bmatrix} A - B\cos(2\theta_r) & 0 & 0 \\ 0 & A - B\cos(2(\theta_r - \frac{2\pi}{3})) & 0 \\ 0 & 0 & A - B\cos(2(\theta_r + \frac{2\pi}{3})) \end{bmatrix} \frac{d}{dt} \begin{bmatrix} i_a \\ i_b \\ i_c \end{bmatrix} \quad (2.4-7)$$

2.5 Electrical Torque

The electrical torque that the variable reluctance stepper motor is capable of developing can be obtained from the partial derivative of the so called coenergy with respect to θ_r . In a linear magnetic system, the coenergy is equal to the energy stored in the magnetic field. From the study of circuit theory, it is known that the energy stored in a system of inductors is

$$E = \frac{1}{2} i^t \underline{L} i. \quad (2.5-1)$$

If we take the partial derivative of EQ (2.5-1) with respect to θ_r , we find the electrical torque is given by

$$T_e = \frac{1}{2} i^t \frac{\partial}{\partial \theta_r} \underline{L} i. \quad (2.5-2)$$

Substituting the a, b, and c phase currents, as well as the expressions for the inductances in each phase into EQ (2.5-2) yields

$$T_e = B \begin{bmatrix} i_a & i_b & i_c \end{bmatrix} \begin{bmatrix} \sin(2\theta_r) & 0 & 0 \\ 0 & \sin(2(\theta_r - \frac{2\pi}{3})) & 0 \\ 0 & 0 & \sin(2(\theta_r + \frac{2\pi}{3})) \end{bmatrix} \begin{bmatrix} i_a \\ i_b \\ i_c \end{bmatrix} \quad (2.5-3)$$

2.6 Shaft Dynamics

If the motor is to turn, a net torque must act to accelerate the rotor, i.e.,

$$T_e - T_l = J \frac{d}{dt} \omega_r + B \omega_r. \quad (2.6-1)$$

In EQ (2.6-1), J is the combined inertia of the rotor and load, and B is a viscous damping coefficient. The torque generated by the motor for a specific operating condition is given by EQ (2.5-3)

2.7 State Variable Model

The goal of this section is to build a state variable model of the variable reluctance motor. The required state variables are the motor currents, rotor angular position and the rotor's angular velocity. EQs (2.4-5), (2.4-7) and (2.6-1) must be solved for the derivatives of the state variables, EQ (2.5-3) is the necessary expression for electrical torque. The matrix differential equation which describes the motor is

$$\frac{d}{dt} \begin{bmatrix} i_a \\ i_b \\ i_c \\ \theta_r \\ \omega_r \end{bmatrix} = - \begin{bmatrix} \frac{v_a}{A - B \cos(2\theta_r)} \\ \frac{v_b}{A - B \cos(2(\theta_r - \frac{2\pi}{3}))} \\ \frac{v_c}{A - B \cos(2(\theta_r + \frac{2\pi}{3}))} \\ 0 \\ \frac{T_l - T_e}{J} \end{bmatrix} + \quad (2.7-1)$$

$$\begin{bmatrix} \frac{r + 2B\omega_r \sin(2\theta_r)}{A - B \cos(2\theta_r)} & 0 & 0 & 0 & 0 \\ 0 & \frac{r + 2B\omega_r \sin(2(\theta_r - \frac{2\pi}{3}))}{A - B \cos(2(\theta_r - \frac{2\pi}{3}))} & 0 & 0 & 0 \\ 0 & 0 & \frac{r + 2B\omega_r \sin(2(\theta_r + \frac{2\pi}{3}))}{A - B \cos(2(\theta_r + \frac{2\pi}{3}))} & 0 & 0 \\ 0 & 0 & 0 & 0 & 1 \\ 0 & 0 & 0 & 0 & \frac{-B}{J} \end{bmatrix} \begin{bmatrix} i_a \\ i_b \\ i_c \\ \theta_r \\ \omega_r \end{bmatrix}$$

CHAPTER 3

THE DQ TRANSFORMATION APPLIED TO A VARIABLE RELUCTANCE STEPPER MOTOR

3.1 Motivation for DQ Analysis

The equation which describes the electrical characteristics of the stepper motor, EQ (2.4-7), is decoupled, i.e., a phase current depends only upon the voltage applied to the phase and the electrical parameters of the phase. Notice however, the inductances in EQ (2.4-7) are time varying. If possible, the time varying terms should be eliminated from this equation and the state equation (2.7-1). The approach taken is to apply the ubiquitous dq transformation developed by RH Park [4]. This change of variables, when applied to synchronous machines, produces a system of differential equations in which the time varying inductances become constants. The similarity between the self-inductance matrix of the variable reluctance motor and the synchronous machine suggests that the transformation may prove useful in this application. In fact, VD Hair [5] has applied the dq transformation to a single stack variable reluctance motor where the coefficients of both the self and mutual inductance are equal.

3.2 DQ Analysis

The equation which implements the dq transformation is

$$f_{qd0} = \underline{K}f_{abc}. \quad (3.2-1)$$

In EQ (3.2-1), f can represent current, voltage or flux linkages. First, a word about notation. Throughout this work, variables subscripted as "abc" refer to machine quantities, i.e., non-transformed variables. Variables which have been transformed to the dq reference frame are identified by the "qd0" subscript. This notation is developed by PC Krause [1]. The transformation is defined as

$$K = \frac{2}{3} \begin{bmatrix} \cos(\theta_r) & \cos(\theta_r - \frac{2\pi}{3}) & \cos(\theta_r + \frac{2\pi}{3}) \\ \sin(\theta_r) & \sin(\theta_r - \frac{2\pi}{3}) & \sin(\theta_r + \frac{2\pi}{3}) \\ \frac{1}{2} & \frac{1}{2} & \frac{1}{2} \end{bmatrix} \quad (3.2-2)$$

The inverse transformation is

$$K^{-1} = \begin{bmatrix} \cos(\theta_r) & \sin(\theta_r) & 1 \\ \cos(\theta_r - \frac{2\pi}{3}) & \sin(\theta_r - \frac{2\pi}{3}) & 1 \\ \cos(\theta_r + \frac{2\pi}{3}) & \sin(\theta_r + \frac{2\pi}{3}) & 1 \end{bmatrix} \quad (3.2-3)$$

In order to see how to apply the dq transformation, EQ (2.4-7) is rewritten symbolically as

$$V_{abc} = R I_{abc} + \frac{d}{dt} \Lambda_{abc} \quad (3.2-4)$$

Applying the transformation to EQ (3.2-4) and premultiplying by K gives

$$V_{qd0} = R I_{qd0} + \omega_r \Lambda_{dq0} + \frac{d}{dt} \Lambda_{qd0} \quad (3.2-5)$$

Note that the flux linkages, Λ , have been transformed so that

$$\Lambda_{qd0} = K \Lambda_{abc} K^{-1}, \quad (3.2-6)$$

and the following definition has been made:

$$\Lambda_{dq0} = \begin{bmatrix} \lambda_d \\ -\lambda_q \\ 0 \end{bmatrix} \quad (3.2-7)$$

It is not surprising that the torque expression is modified by the application of the dq transformation to our model. The modified torque expression is

$$T_e = \frac{1}{2} I_{qd0}^t (K^{-1})^t \frac{\partial}{\partial \theta_r} L K^{-1} I_{qd0} \quad (3.2-8)$$

or equivalently

$$T_e = \frac{3}{2} B \begin{bmatrix} i_q & i_d & i_0 \end{bmatrix} \begin{bmatrix} 0 & \frac{1}{2} & \sin 3\theta_r \\ \frac{1}{2} & 0 & -\cos 3\theta_r \\ \sin 3\theta_r & -\cos 3\theta_r & 0 \end{bmatrix} \begin{bmatrix} i_q \\ i_d \\ i_0 \end{bmatrix} \quad (3.2-9)$$

Excluding the changes made to the electrical torque expression just discussed,

EQ (2.6-1), the relation for shaft dynamics, is unaffected by the dq transformation.

3.3 Effect of the DQ Transformation on Flux Linkages

The stated goal of the previous section was to obtain a time-invariant matrix equation which would describe the electrical behavior of the variable reluctance motor. The new flux linkage matrix is

$$\Lambda_{qdo} = \begin{bmatrix} \lambda_q \\ \lambda_d \\ \lambda_o \end{bmatrix} = \begin{bmatrix} \frac{1}{2}(2A - B) & 0 & -B\cos 3\theta_r \\ 0 & \frac{1}{2}(2A + B) & -B\sin 3\theta_r \\ -\frac{1}{2}B\cos 3\theta_r & -\frac{1}{2}B\sin 3\theta_r & A \end{bmatrix} \begin{bmatrix} i_q \\ i_d \\ i_o \end{bmatrix} \quad (3.3-1)$$

The desired result *has not* been obtained; the flux linkage matrix still contains time varying terms in the third row and third column.

Certain problems in electric machine analysis have been made more amenable to solution by averaging techniques. One example of the application of such techniques is in the analysis of unbalanced stator voltages applied to a two phase induction motor. In that analysis [6], positive and negative sequence currents are used to compute positive and negative sequence torque. A so called "pulsating torque" also exists under these operating conditions. The torque-speed curves for such a device are adequately represented by averaging the positive sequence, negative sequence and pulsating torque. This average torque is expressed as

$$T_{e(ave)} = T_{e+} - T_{e-} \quad (3.3-2)$$

In the above expression, the pulsating torque is not included since it has an average value of zero.

An averaging technique will be applied to the flux linkage matrix of EQ (3.3-1). If it is assumed that i_q , i_d and i_o are dc, the sinusoidal, off-diagonal terms will contribute an average value of zero, so the averaged flux linkages become

$$\bar{\Lambda}_{qdo} = \begin{bmatrix} \bar{\lambda}_q \\ \bar{\lambda}_d \\ \bar{\lambda}_o \end{bmatrix} = \begin{bmatrix} \frac{1}{2}(2A - B) & 0 & 0 \\ 0 & \frac{1}{2}(2A + B) & 0 \\ 0 & 0 & A \end{bmatrix} \begin{bmatrix} i_q \\ i_d \\ i_o \end{bmatrix} \quad (3.3-3)$$

If the currents are not dc, the above formulation will not give the correct average flux linkages; however, inclusion of the necessary terms to give the

correct result would produce a non-diagonal flux linkage matrix. This is undesirable, so the above formulation will be used regardless of the form of the model currents. Notice that this *is not* the inductance matrix that would have been obtained had the abc flux linkages been averaged, nor is it the inductance matrix commonly found in dq analysis of synchronous machines.

3.4 Transformed Voltage Equations

The matrix differential equations describing the electrical circuits of the motor will be presented in this section. When the inductance matrix is not averaged, the expressions for the derivatives of the qd0 currents are quite involved. For this reason, the voltage equations will not be solved explicitly for these currents, rather, the equations will be shown as

$$\begin{bmatrix} v_q \\ v_d \\ v_o \end{bmatrix} = \begin{bmatrix} r & \frac{\omega_r}{2}(2A+B) & 0 \\ -\frac{\omega_r}{2}(2A-B) & r & 0 \\ 0 & 0 & r \end{bmatrix} \begin{bmatrix} i_q \\ i_d \\ i_o \end{bmatrix} + \frac{1}{2} B \omega_r \begin{bmatrix} 0 & 0 & 4\sin 3\theta_r \\ 0 & 0 & -4\cos 3\theta_r \\ 3\sin 3\theta_r & -3\cos 3\theta_r & 0 \end{bmatrix} \begin{bmatrix} i_q \\ i_d \\ i_o \end{bmatrix} + \frac{1}{2} \begin{bmatrix} 2A-B & 0 & -2B\cos 3\theta_r \\ 0 & 2A+B & -2B\sin 3\theta_r \\ -B\cos 3\theta_r & -B\sin 3\theta_r & 2A \end{bmatrix} \frac{d}{dt} \begin{bmatrix} i_q \\ i_d \\ i_o \end{bmatrix} \quad (3.4-1)$$

In this form, the dq transformation has not brought about much computational simplicity.

The equations which make use of the averaged inductance matrix are considerably simplified. The voltage equation becomes

$$\begin{bmatrix} v_q \\ v_d \\ v_o \end{bmatrix} = \begin{bmatrix} r & \frac{\omega_r}{2}(2A+B) & 0 \\ -\frac{\omega_r}{2}(2A-B) & r & 0 \\ 0 & 0 & r \end{bmatrix} \begin{bmatrix} i_q \\ i_d \\ i_o \end{bmatrix} + \frac{1}{2} \begin{bmatrix} 2A-B & 0 & 0 \\ 0 & 2A+B & 0 \\ 0 & 0 & 2A \end{bmatrix} \frac{d}{dt} \begin{bmatrix} i_q \\ i_d \\ i_o \end{bmatrix} \quad (3.4-2)$$

Unlike EQ (3.4-1), it is easy to solve for the derivatives of current in EQ (3.4-2). The state equation for the case of averaged flux linkages is

$$\frac{d}{dt} \begin{bmatrix} i_q \\ i_d \\ i_o \\ \theta_r \\ \omega_r \end{bmatrix} = \begin{bmatrix} \frac{2v_q}{2A-B} \\ \frac{2v_d}{2A+B} \\ \frac{v_o}{A} \\ 0 \\ \frac{T_1 - T_e}{J} \end{bmatrix} + \quad (3.4-3)$$

$$\begin{bmatrix} \frac{-2r}{2A-B} & \frac{-\omega_r(2A+B)}{2A-B} & 0 & 0 & 0 \\ \frac{\omega_r(2A-B)}{2A+B} & \frac{-2r}{2A+B} & 0 & 0 & 0 \\ 0 & 0 & -\frac{r}{A} & 0 & 0 \\ 0 & 0 & 0 & 0 & 1 \\ 0 & 0 & 0 & 0 & -\frac{B}{J} \end{bmatrix} \begin{bmatrix} i_q \\ i_d \\ i_o \\ \theta_r \\ \omega_r \end{bmatrix}$$

The matrix differential equation has been simplified by the change of variables. Time varying elements in the electrical portion of the state model have been eliminated, however, the equation is still non-linear.

One particularly interesting property of the "averaged" state equation is apparent. For a constant speed solution in the steady state, the q, d and 0 currents can be found without use of numerical integration. The steady state assumption implies that the derivatives of the currents are zero, hence, the steady state currents in EQ (3.4-3) can be found using the relation

$$\begin{bmatrix} i_q \\ i_d \\ i_o \end{bmatrix} = - \begin{bmatrix} \frac{-2r}{2A-B} & \frac{-\omega_r(2A+B)}{2A-B} & 0 \\ \frac{\omega_r(2A-B)}{2A+B} & \frac{-2r}{2A+B} & 0 \\ 0 & 0 & -\frac{r}{A} \end{bmatrix}^{-1} \begin{bmatrix} \frac{2v_q}{2A-B} \\ \frac{2v_d}{2A+B} \\ \frac{v_o}{A} \end{bmatrix} \quad (3.4-4)$$

CHAPTER 4 COMPARISON OF RESULTS FOR DETAILED AND AVERAGE DQ SIMULATION

4.1 Introduction

In this chapter, continuous operation of a variable reluctance stepper motor will be examined. In particular, a motor will be simulated using the equations which were obtained from the dq analysis. The results of this simulation will be compared with those obtained using the "averaged" inductance matrix. Machine currents, represented in qd0 variables will be shown, and plots of machine torque will be presented. These results were obtained via a numerical integration procedure. This procedure is the subject of the section to follow.

4.2 Numerical Integration

Essentially, the problem at hand deals with the solution of

$$\dot{X} = F(X(t), t) \tag{4.2-1}$$

via numerical techniques. One approach to solving such a problem uses what are termed predictor methods to evaluate the integral. The fourth order Runge-Kutta method is one such scheme. It is interesting to note that this scheme requires four functional evaluations to obtain an estimate for a new state. Alternatively, a so called predictor-corrector method can be employed. With such a method, previous state vectors are used to estimate the value of the new state vector. This new vector is used to re-evaluate the function. The estimate is then adjusted appropriately, and the process continues. While a predictor method may only require one new functional evaluation per integration step, the value of the function at several successive time instants must be known. The approach taken in the simulations employed in this thesis is to use the fourth order Runge-Kutta method to generate four state estimates. Once the state vectors at these initial time instants are known, the Adams-Bashforth predictor-corrector method is used to compute the

remaining state estimates. A more detailed discussion of these topics can be found in [7] and [8].

4.3 Device Parameters and Mode of Operation

The simulations in this thesis deal with constant speed operation. In other words, it is desired to have the rotor turning continuously rather than moving in discrete steps. A need for this type of motion may arise in a line printer where a form feed is requested. Alternatively, the application could be a computer disc drive where it is necessary to move the head to a new, relatively distant, sector of the disc. In these applications, the accurate positioning capability of the motor is not needed. What is needed is to move quickly to a new position where the stepping capabilities of the motor will be used. The motor will be studied in this mode. Except where noted, the system parameters found in Table 4.1 are those used throughout this work.

4.4 Currents at Constant Speed

In the studies which follow, the motor is supplied by a bipolar drive circuit of the type described in Chapter 2. The motor is assumed to be rotating at its base speed of 377 rad/s, and the rotor angle, δ , is held at 0° . Fig - 4.1 shows the q, d, and 0 currents obtained from the machine simulation with the detailed inductance matrix. The motor has reached steady state, and we see that there is a sinusoidal variation about an average value in each of the currents. This is to be compared with the currents shown in Fig - 4.2 which were obtained by running a simulation which makes use of the average inductance matrix. The average values of i_q , i_d , and i_0 obtained from the detailed qd0 simulation are compared with the values from averaged simulation in Table 4 - 2. It is seen that the averaged model has predicted the average value of the machine currents quite accurately. The reason for the discrepancy in average currents will be explained in the section which follows.

Table 4.1 Motor parameters.

PARAMETER	SYMBOL	VALUE
Base Voltage	V_B	24.0 V
Base Current	I_B	0.6 A
Base Torque	T_B	38.2 N*mm
Base Speed	ω_B	377 rad/s
Stator Resistance	R	20 Ω
Inertia	J	12.7 g cm ²
Inductance constant A	A	0.050 H
Inductance constant B	B	0.019 H

Table 4.2 Comparison of machine currents.

CURRENT	AVE. FIG 4.1	AVE. FIG 4.2	% DIFF.
\bar{i}_q	0.424	0.412	2.8
\bar{i}_d	0.307	0.314	-2.3
\bar{i}_0	0.0	0.0	0.0

Table 4.3 Comparison of machine torques.

TORQUE (N*cm)	AVE. FIG 4.3	AVE. FIG 4.4	% DIFF.
\bar{T}_e	0.32	0.37	-15.6

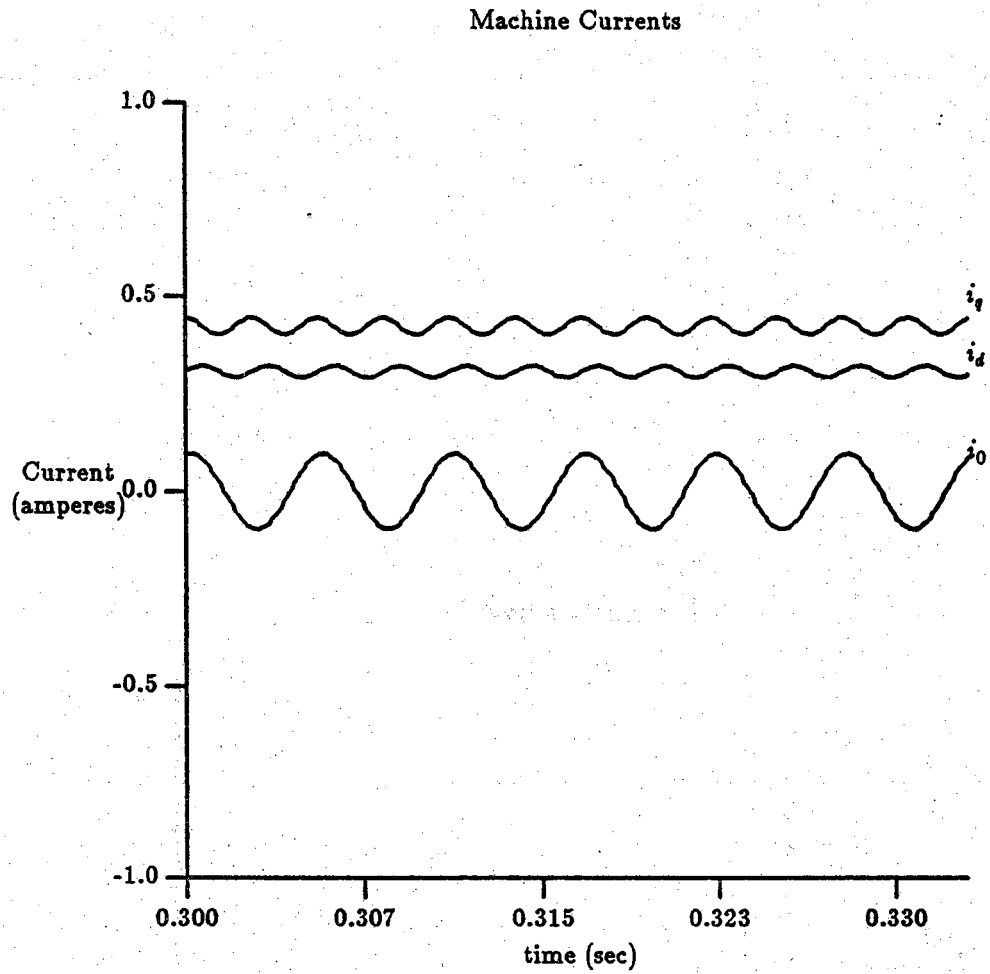


Figure 4.1 Machine currents (steady state, detailed inductance matrix).

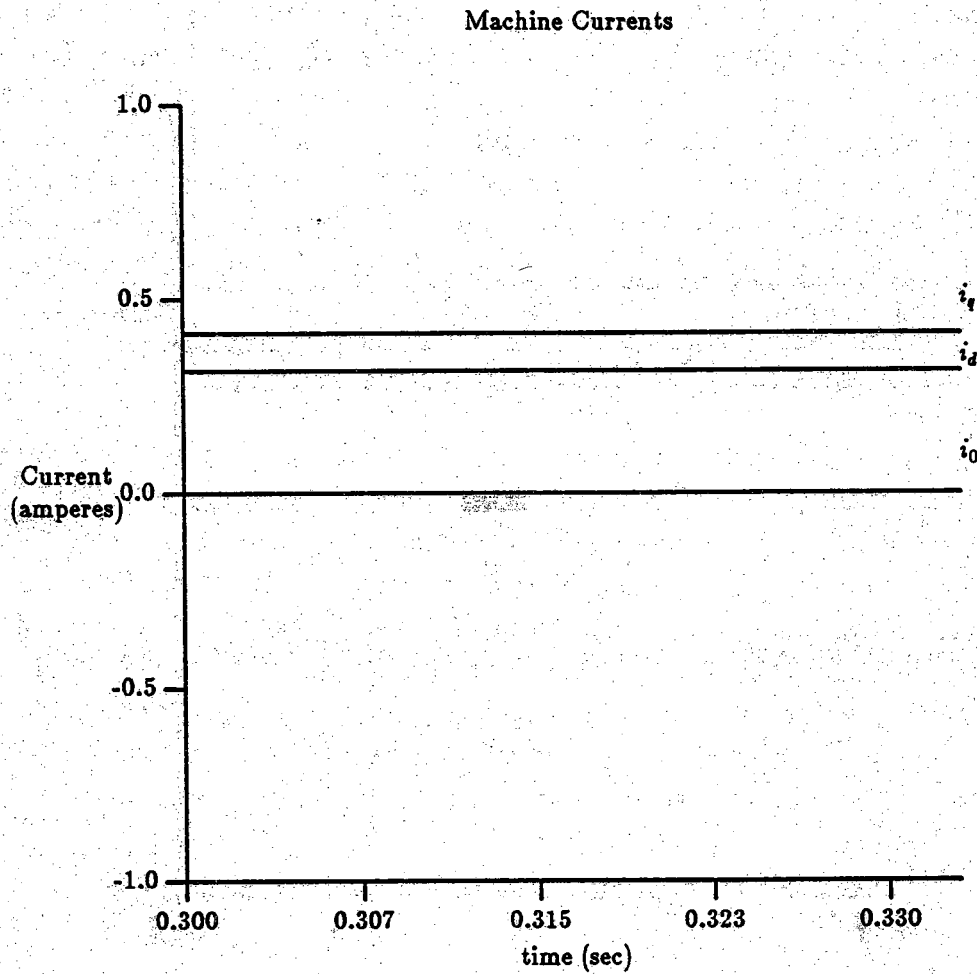


Figure 4.2 Machine currents (steady state, averaged inductance matrix).

4.5 Machine Torques

The truly useful feature of any electric motor is its ability to produce a torque. Therefore, it is only natural that a comparison should be made between the torque obtained from a simulation which makes use of an averaged inductance matrix and one which does not. When the state model with the detailed inductance matrix is employed, the torque shown in Fig - 4.3 is obtained. An average and sixth harmonic of torque are clearly seen. The torque obtained using the averaged model is shown in Fig - 4.4. As is expected, there are no oscillations present in the plot. Table 4 - 3 compares the average torques obtained through use of the two models. The difference in average torque is somewhat unexpected since the agreement between models for the machine currents was much closer. The source of this difference can be found in the expression for torque given in EQ (3.2-9). If this equation is expanded, the following result is obtained:

$$T_e = \frac{3}{2}B(i_q i_d + 2i_q i_0 \sin 3\theta_r - 2i_d i_0 \cos 3\theta_r). \quad (4.5-1)$$

Notice that EQ (4.5-1) contains terms in which i_0 is modulated by terms involving $\sin 3\theta_r$ and $\cos 3\theta_r$. These products will produce components of torque which are at dc and sixth harmonic. Clearly, it is the third harmonic present primarily in i_0 which in this case reduced the average value of the torque. Also, this same interaction gives the sixth harmonic fluctuation which is present in the torque obtained from the detailed state model. A similar interaction occurs with the machine currents expressed in qd0 variables. The third harmonic current in i_0 interacts with terms that vary sinusoidally with $3\theta_r$ to produce an average value and a sixth harmonic variation.

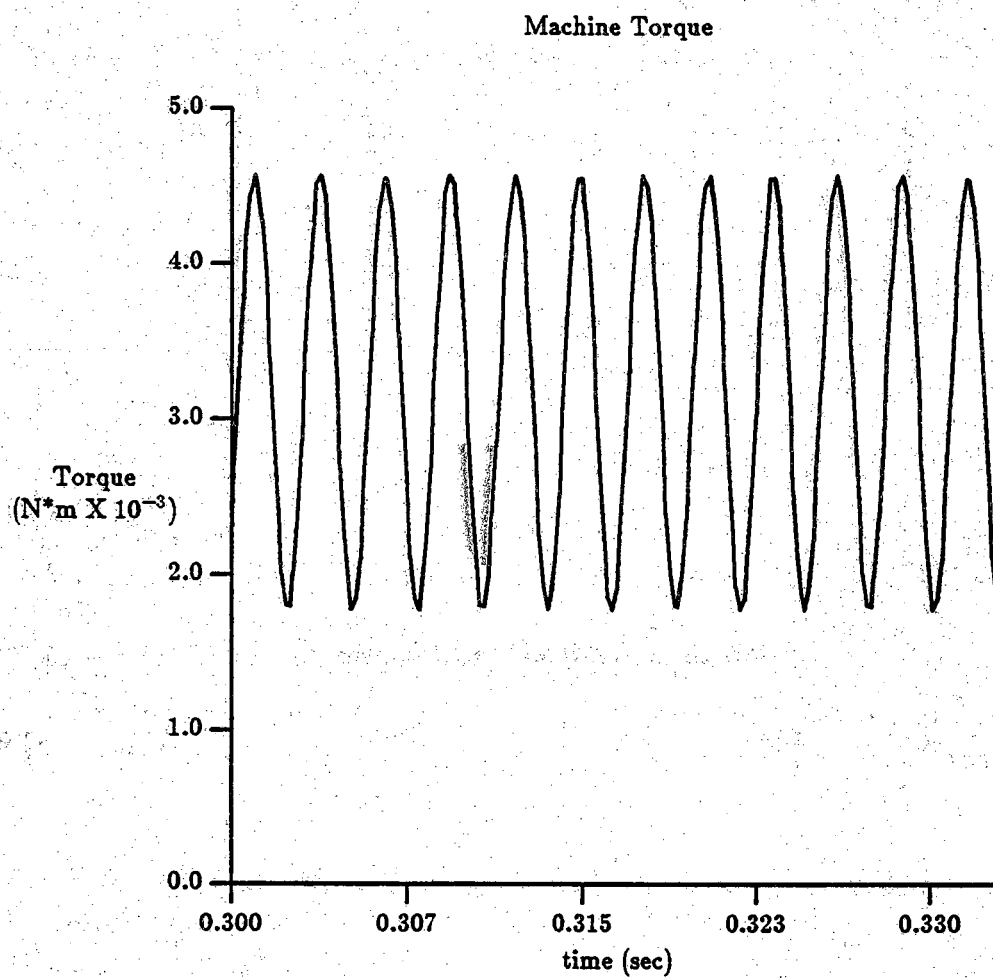


Figure 4.3 Machine torque from the detailed model.

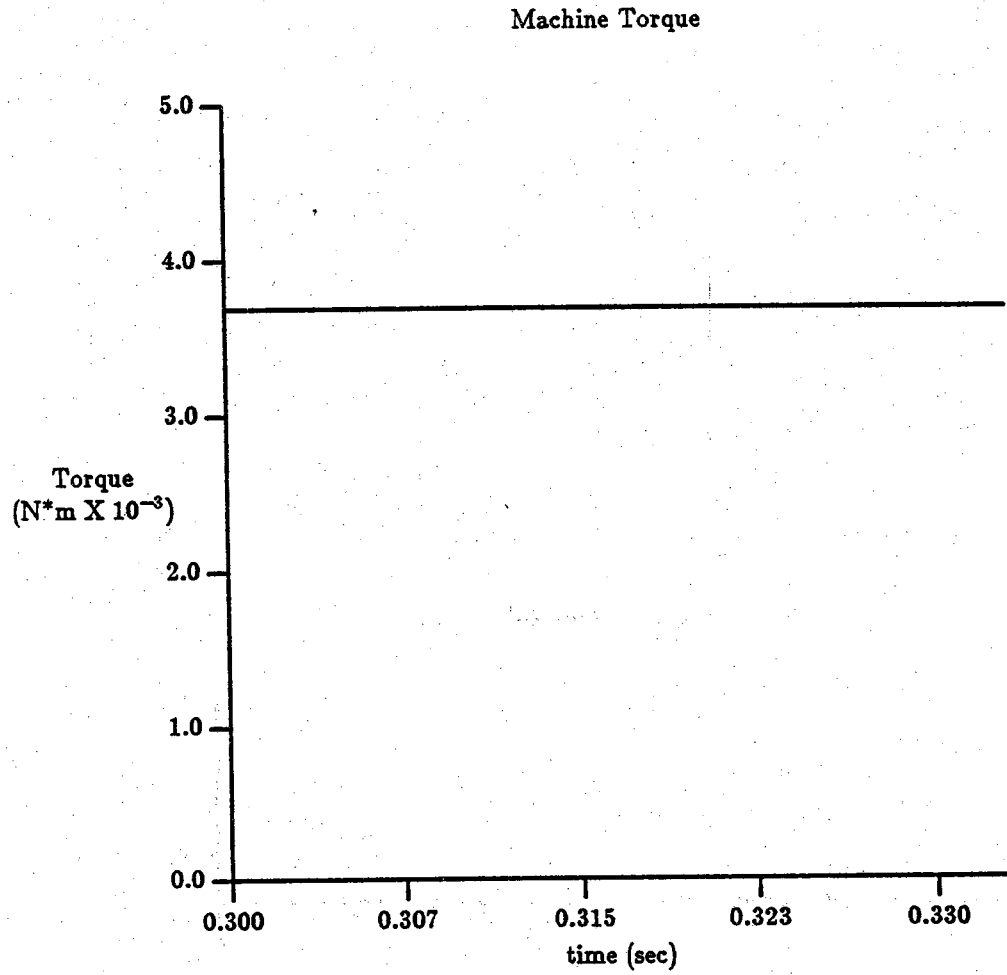


Figure 4.4 Machine torque from the averaged model.

CHAPTER 5 APPLICATIONS OF THE AVERAGE MODEL

5.1 Introduction

In this chapter, certain applications are simulated and a comparison is made between the detailed and average dq model. First, however, the effect of a change in motor parameters, namely resistance, is investigated. Both models are then used to generate plots of torque as a function of rotor angle, δ . Finally, the motor is simulated running at base speed when a step change in load torque is applied.

5.2 Impact of a Change in Motor Resistance on Average Torque

Model efficacy as electrical parameters are changed is to be studied. In particular, the impact of a change in resistance will be examined in the section which follows. The stator resistance of the motor was increased by a factor of 10 to 200 Ω , and the simulations were rerun. The results are shown in the following figures.

The average currents and torque obtained from the two state models are shown in Table 5.1.

Table 5.1 Comparison of state models.

PARAM.	DETAILED. SIM.	AVE. SIM.	% DIFF.
\bar{i}_q	75.69 mA	75.75 mA	-0.07
\bar{i}_d	5.76 mA	5.78 mA	-0.46
\bar{i}_0	0.0 mA	0.0 mA	0.0
\bar{T}_e	4.2 μ Nm	12.5 μ Nm	-200

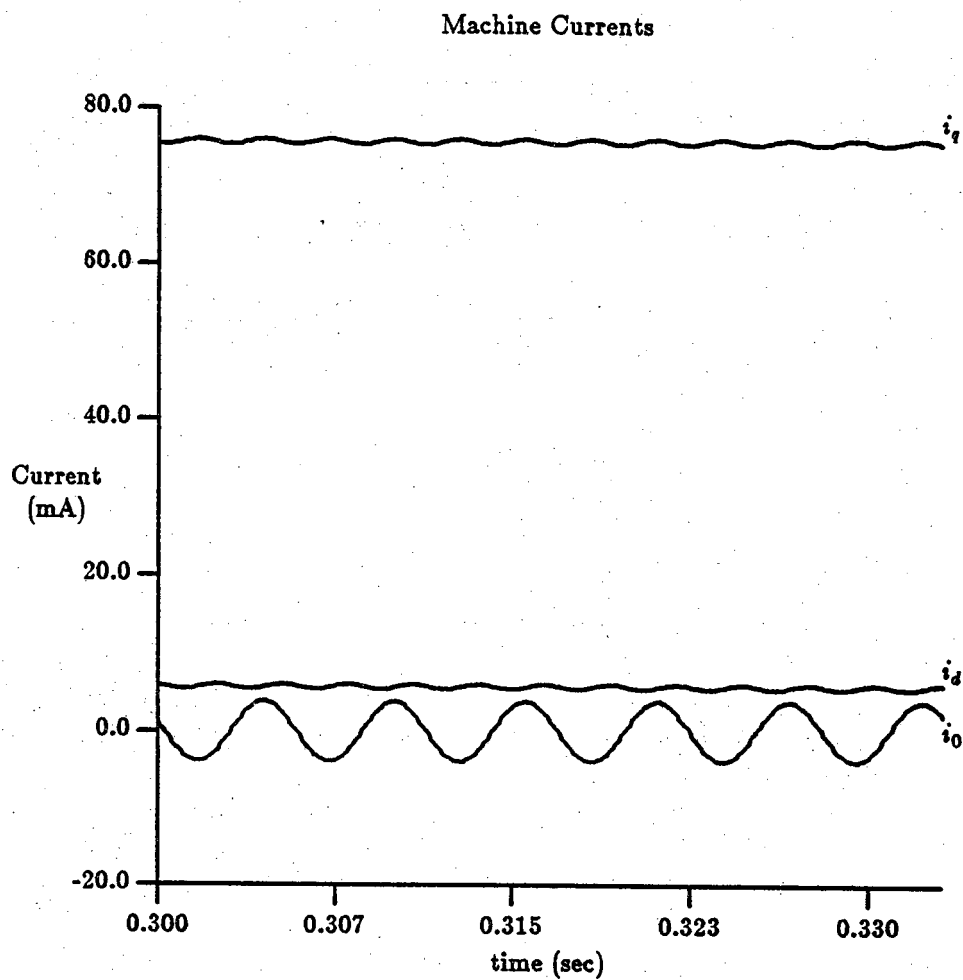


Figure 5.1 Machine currents (detailed model, $R = 200 \Omega$).

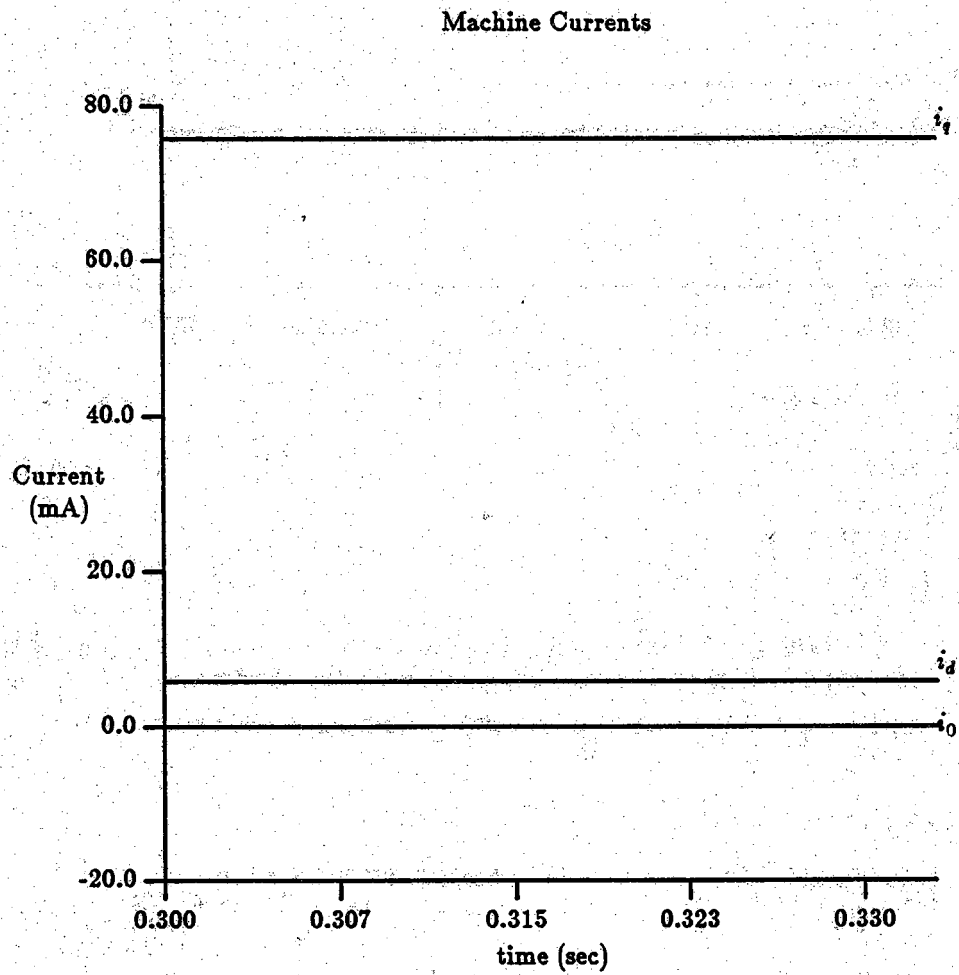


Figure 5.2 Machine currents (averaged model, $R = 200 \Omega$).

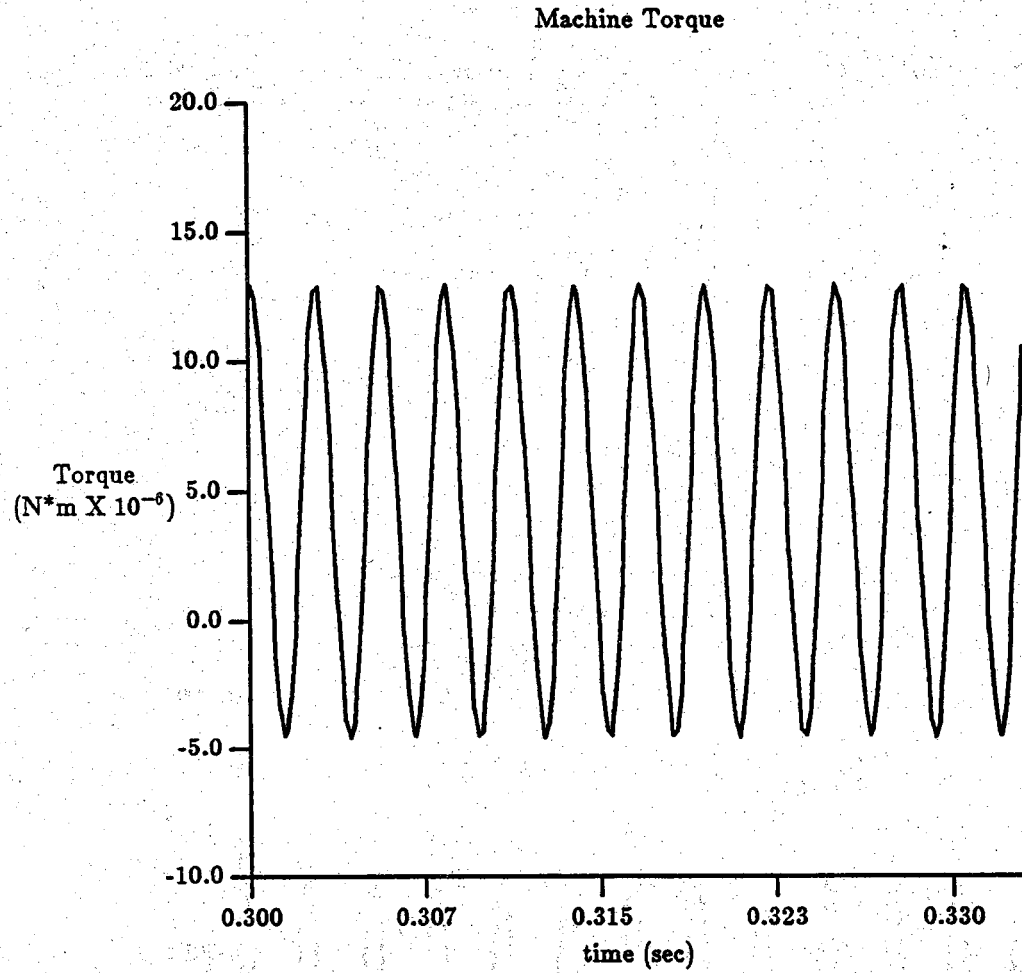


Figure 5.3 Machine torque from the detailed model ($R = 200 \Omega$).

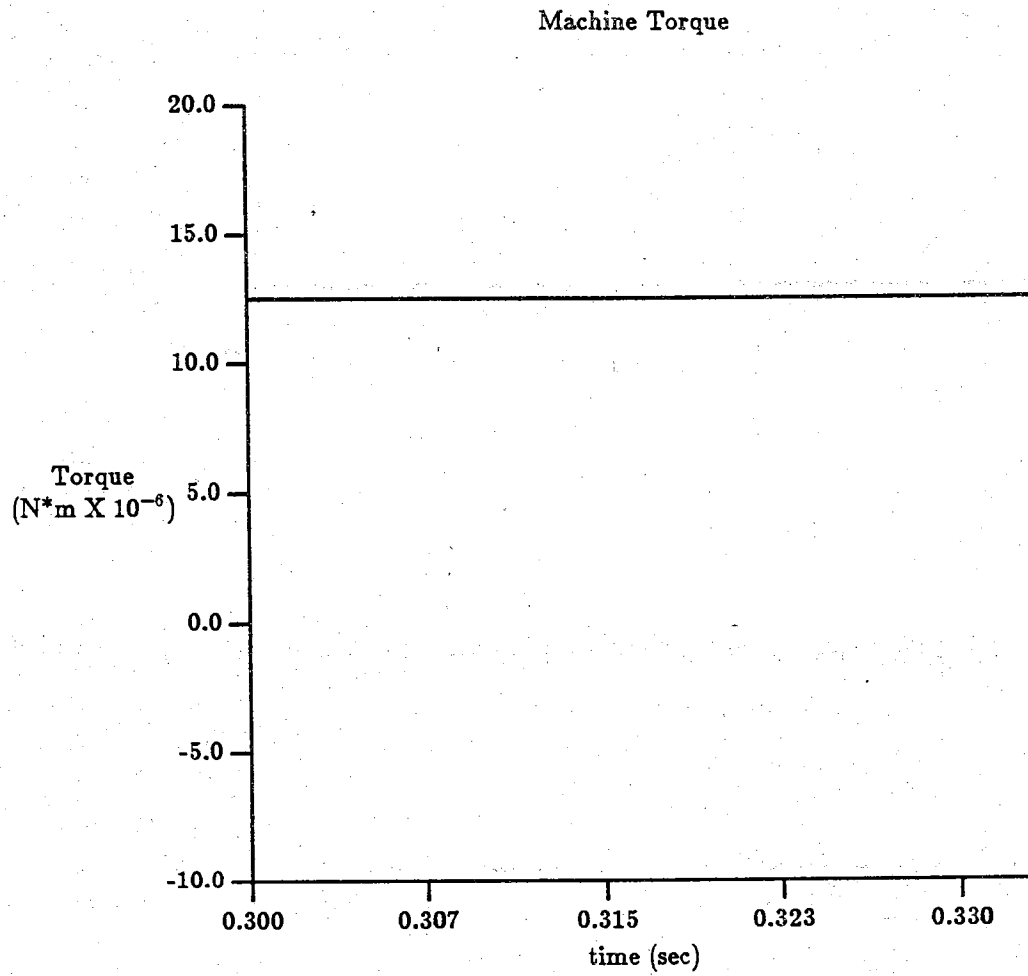


Figure 5.4 Machine torque from the averaged model ($R = 200 \Omega$).

Although the estimates of the machine currents have improved, the torque estimate has been made much worse. The magnitude of the torque oscillations in Fig - 5.3 is large enough to reduce the average value well below that predicted by the averaged model. This suggests that it may not be possible to obtain good results from the average model for all types of variable reluctance stepper motors.

5.3 Torque Delta Curves

The next step in model verification is to simulate both the electrical and mechanical operation of the system. Before this is done however, it is instructive to learn how the torque the motor can develop will change as the rotor angle, δ , changes. Additionally, an indication of the maximum torque the motor can produce will be obtained. Recall from Chapter 2 that a 180 degree change in rotor position produces a magnetic circuit which is identical to that present before the rotation occurred. Accordingly, it is expected that torque will be periodic in δ with period of π . From the study of synchronous machines, one would expect that the torque variation would in fact be sinusoidal. Fig - 5.5 shows the variation in torque as a function of delta for the detailed dq model, while Fig - 5.6 shows the same variation obtained from the average model. Each of these figures shows a torque vs. δ curve for several different rotor speeds.

As expected, the torque - δ curve is sinusoidal. Also, the maximum torque produced by the average model is larger than that produced by the detailed model. This is not unexpected in light of the constant speed results of the previous chapter.

5.4 Dynamic Simulation - Steady State

The variable reluctance motor was next simulated with the mechanical dynamics included. In order to reduce speed oscillations, a damping term was introduced. The value of the damping coefficient used is $8\mu\text{N}^*\text{m}^*\text{sec}$; at 377 rad/sec, a torque of

$$T_1 = 3.02 \times 10^{-3} \text{N}^*\text{m}$$

is applied. Results from simulation of the detailed model are shown in Fig - 5.7 through Fig - 5.10; simulation results obtained using the averaged model are shown in Fig - 5.11 and Fig - 5.12.

Torque vs. δ
detailed simulation

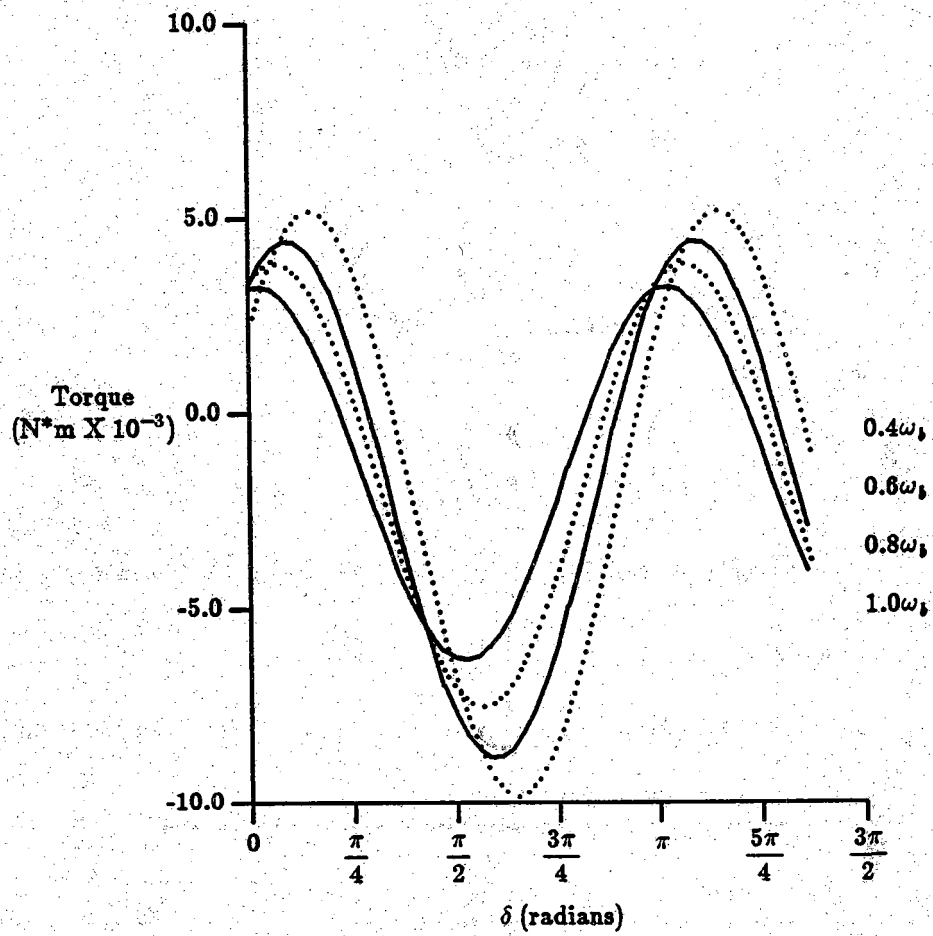


Figure 5.5 Machine torque vs. δ (detailed model).

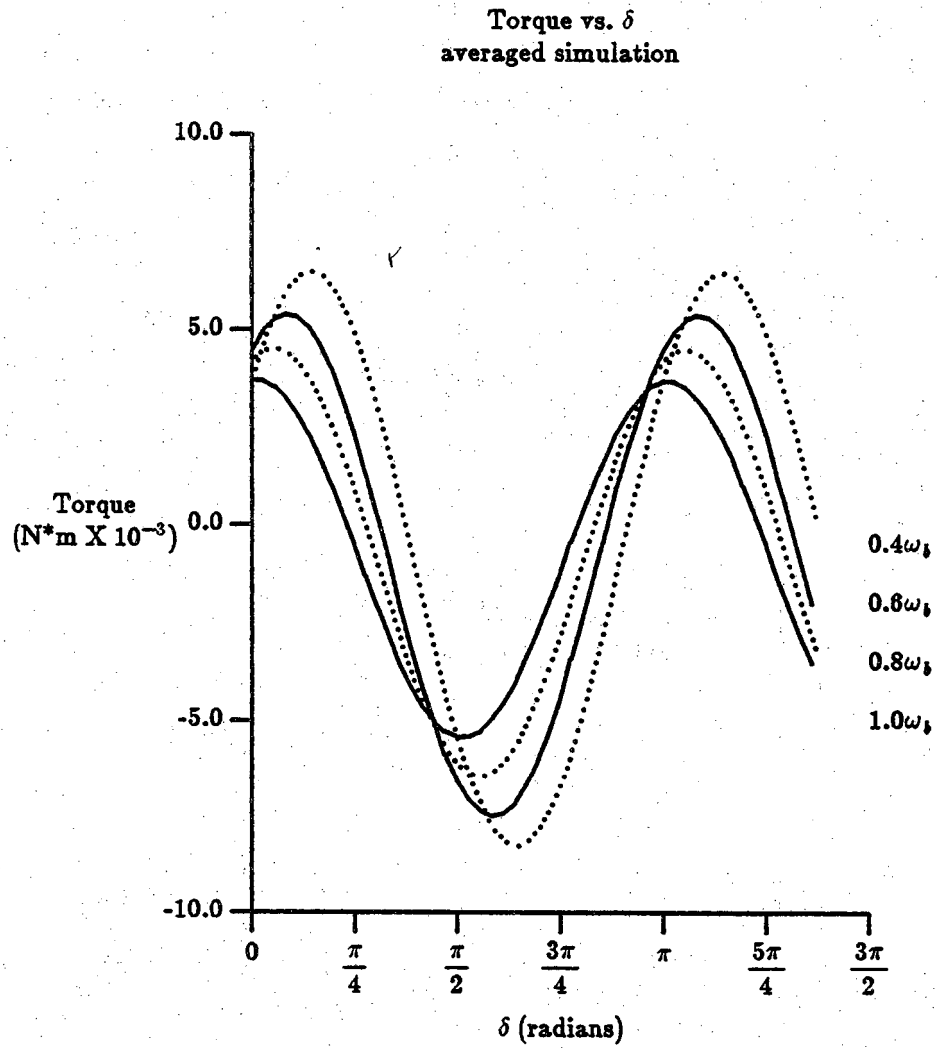


Figure 5.6 Machine torque vs. δ (averaged model).

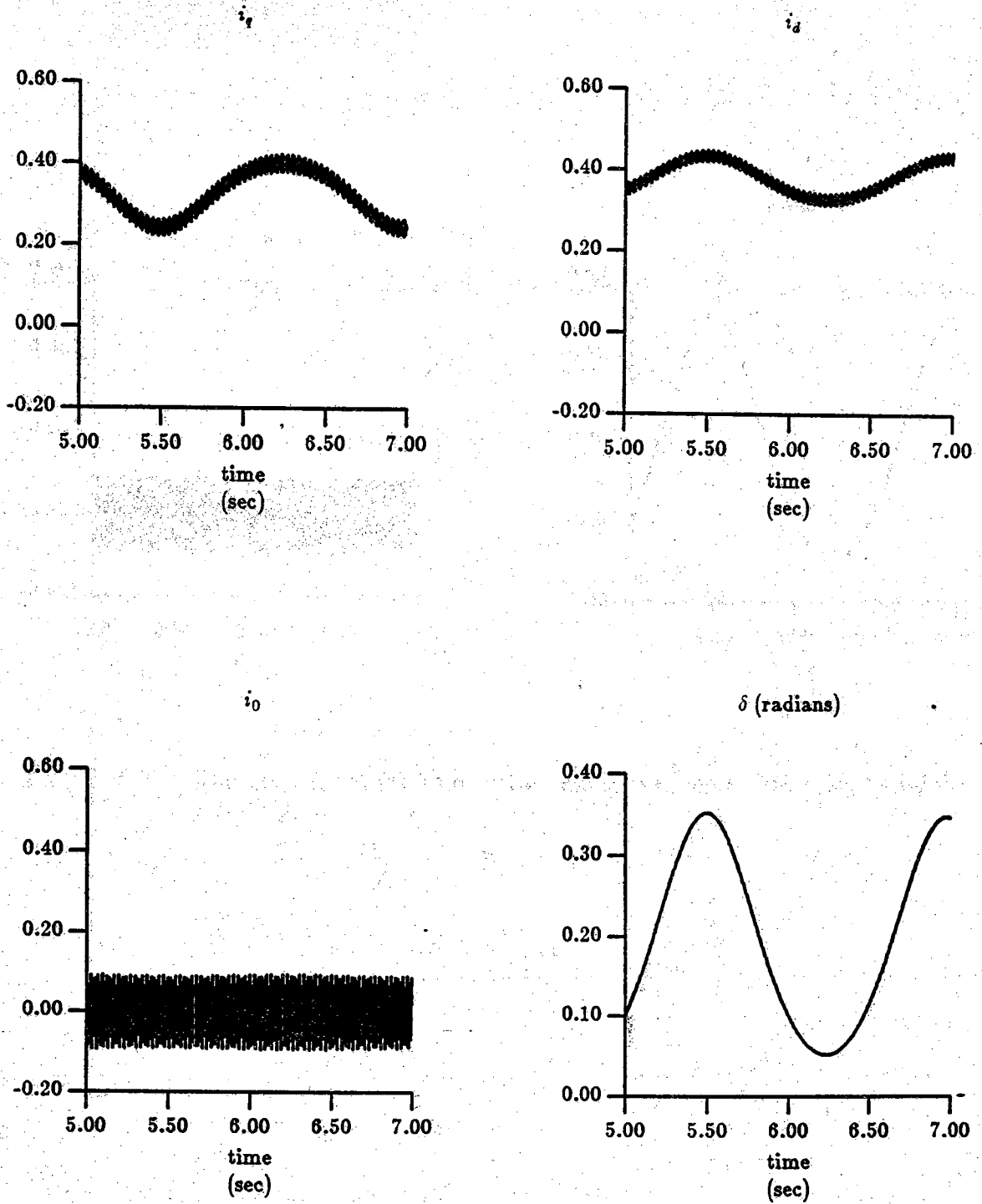


Figure 5.7 Machine currents and rotor angle vs. time (detailed model, damping only).

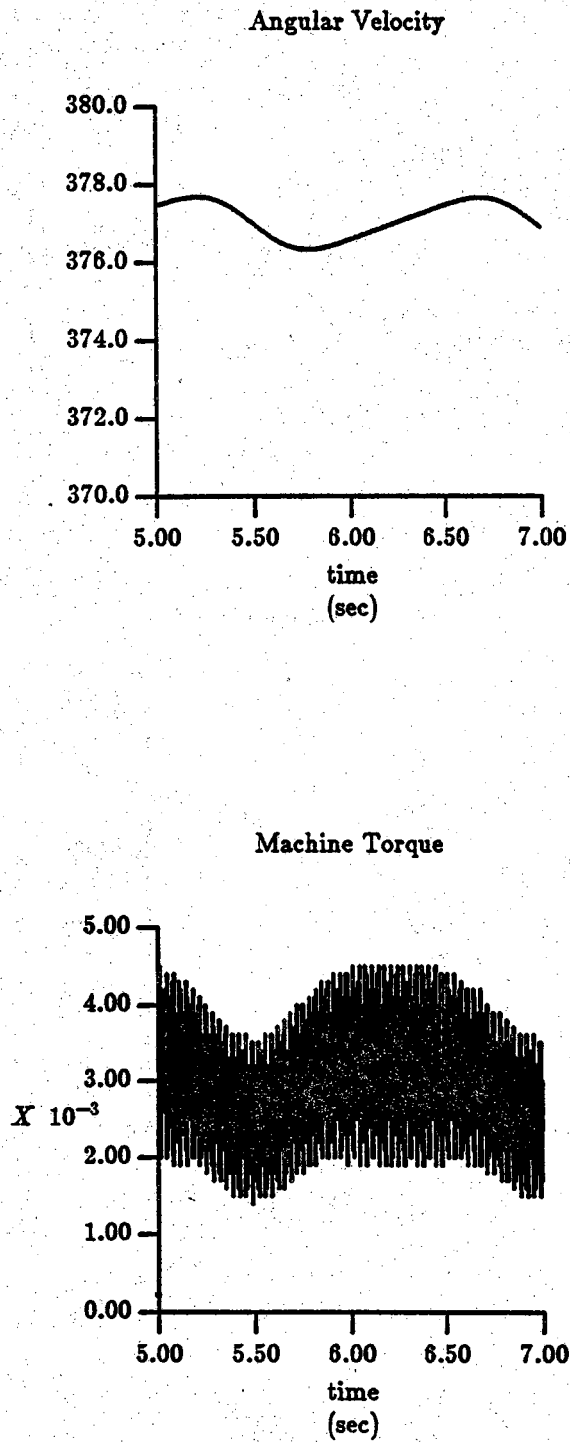


Figure 5.8 Angular velocity and machine torque vs. time (detailed model, damping only).

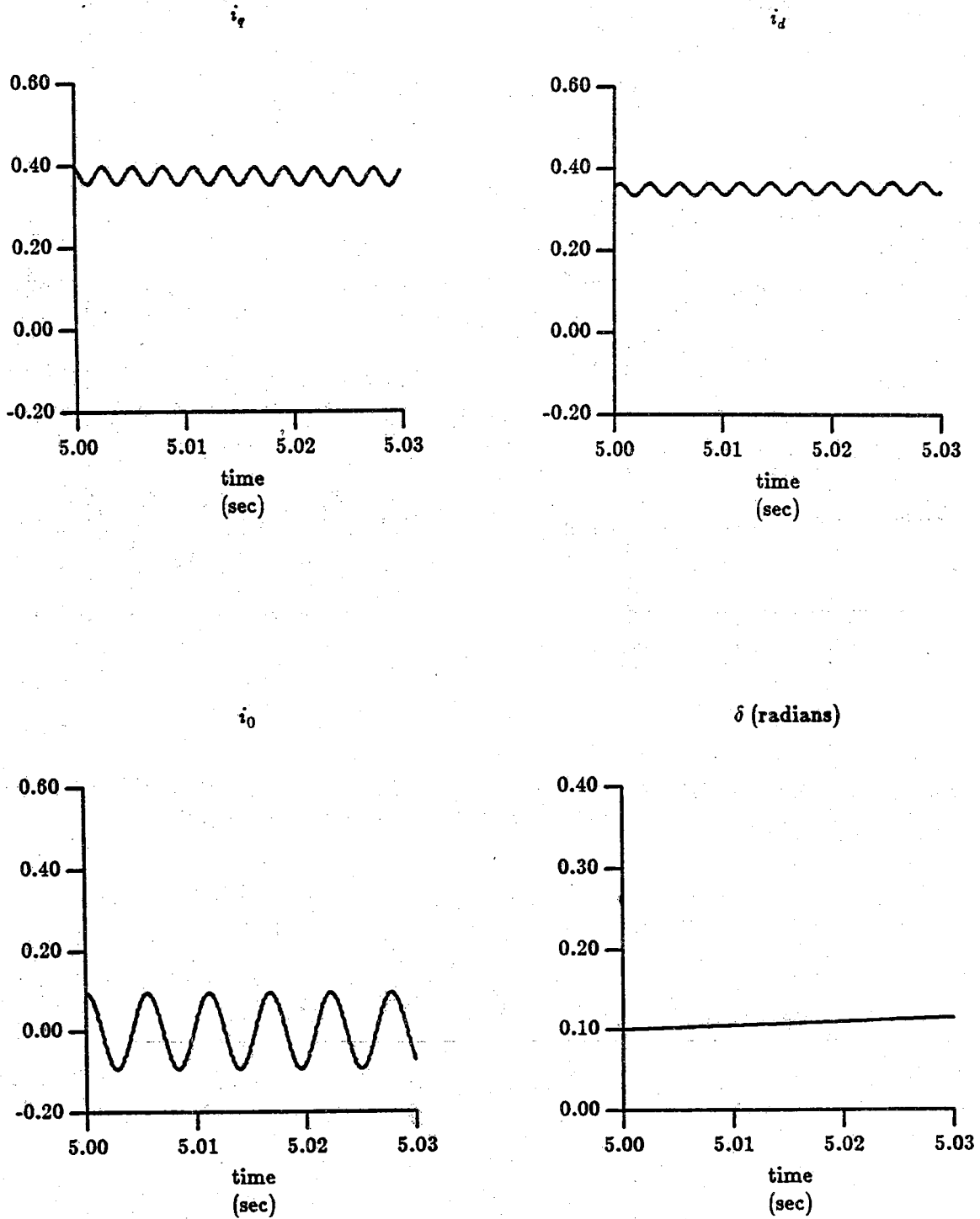


Figure 5.9 Machine currents and rotor angle vs. time (detailed model, expanded time scale, damping only).

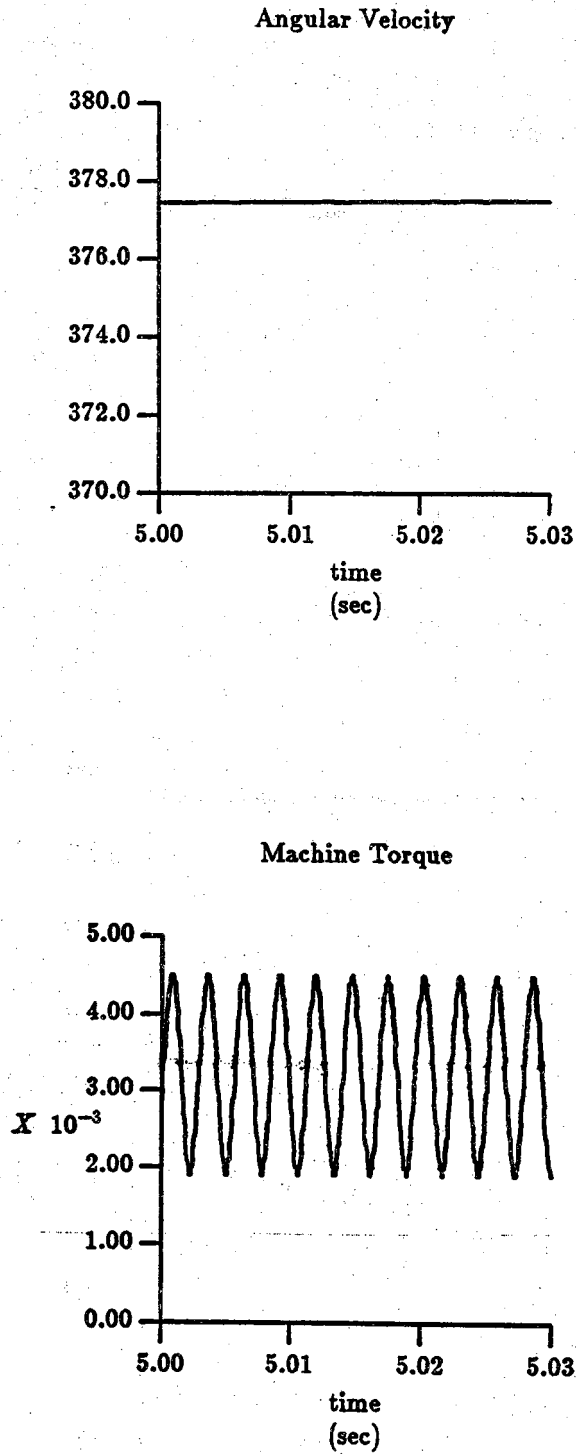


Figure 5.10 Angular velocity and machine torque vs. time (detailed model, expanded time scale, damping only).

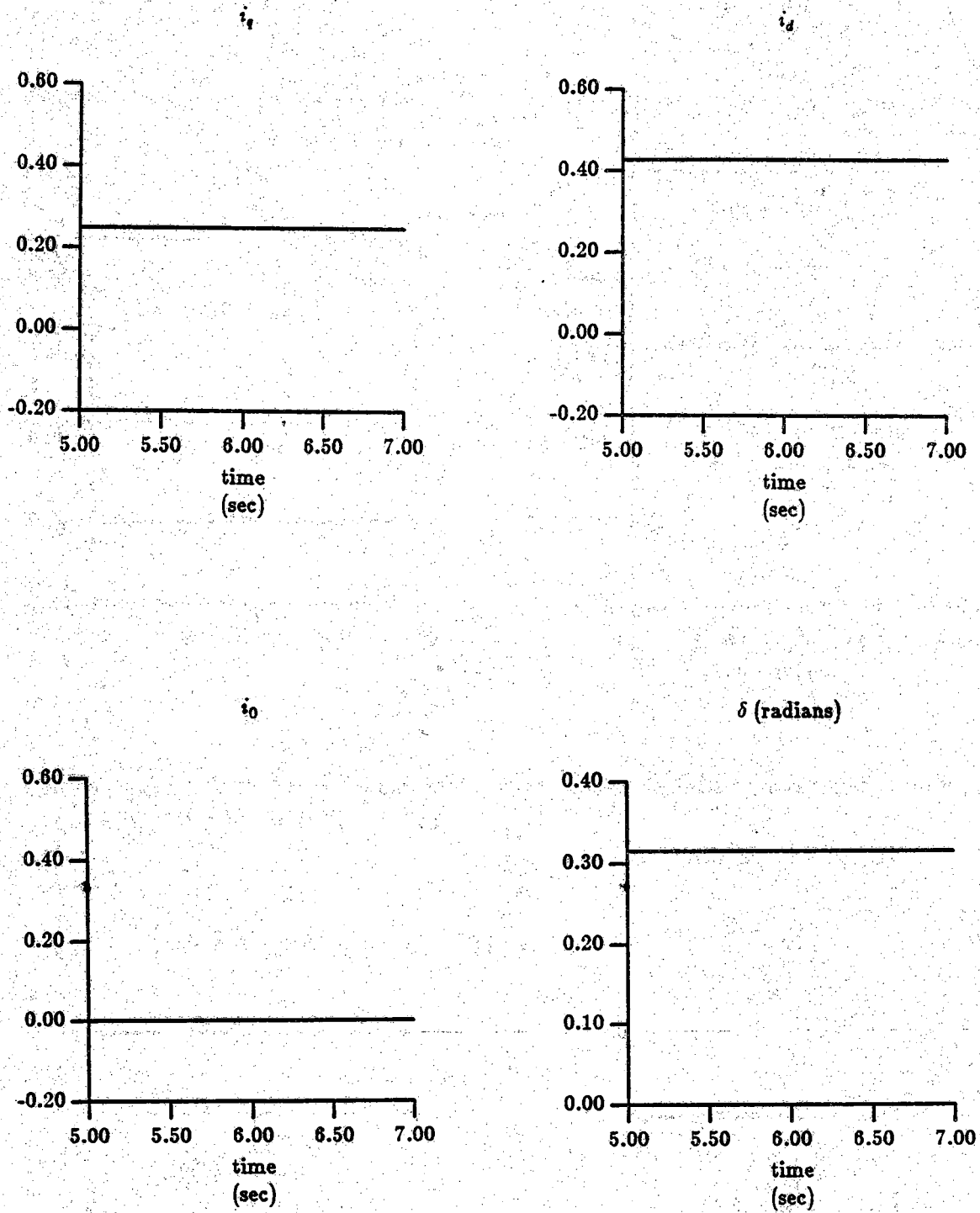
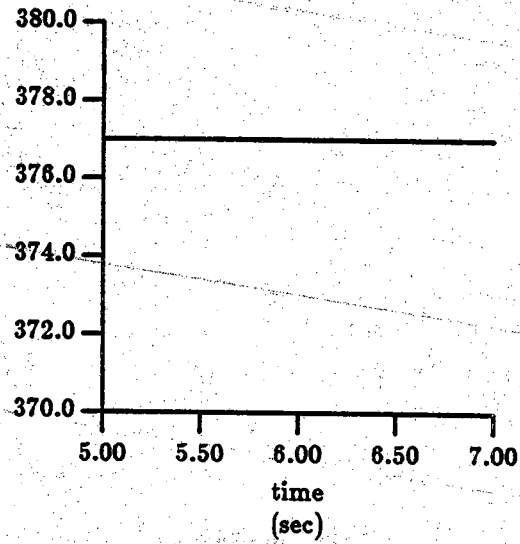


Figure 5.11 Machine currents and rotor angle vs. time (averaged model, damping only).

Angular Velocity



Machine Torque

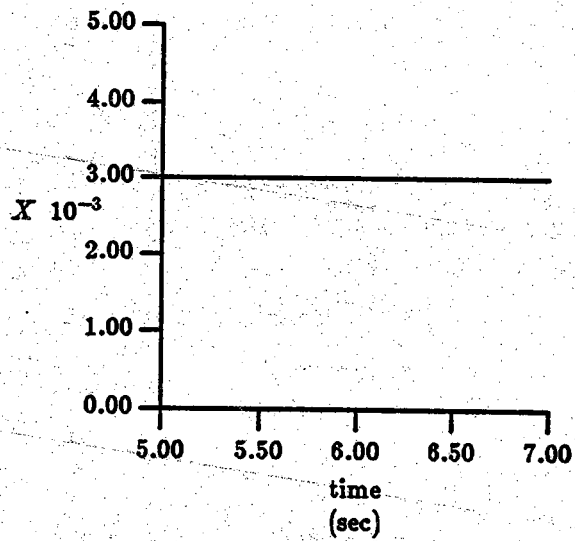


Figure 5.12 Angular velocity and machine torque vs. time (averaged model, damping only).

The steady state dynamic simulation using the average model gives results quite similar to those obtained in Chapter 4. When the detailed model is used for the steady state dynamic simulation, some unexpected results are found. First, notice that the rotor angle oscillates at a frequency of 0.68Hz. In fact, an oscillation is observed in all the machine variables. It is interesting to notice that while the form of machine currents agrees with that of Chapter 4, e.g., i_q is primarily dc with a sixth harmonic oscillation, the magnitude of the dc portion of waveform is no longer accurately predicted by the average model. In general, the results of these simulations agree with those of the proceeding chapter. The average model gives constant currents and torques, while a sixth harmonic is present in i_q , i_d and torque when they are obtained from the detailed model. I_0 is found to be primarily third harmonic.

Since the results of the dynamic simulation are somewhat unexpected, a means of verifying that the simulation gives the correct results is needed. There are two methods which can be used to check the simulation. First, the torque vs. δ curves can be used to predict the rotor angle which is necessary to meet the load torque requirements. Second, it is expected that the currents and torque should be similar to those found in Chapter 4 when only the electrical system was simulated. Table 5.2 compares the rotor angles obtained from the two simulations with those predicted from Fig - 5.5 and Fig - 5.6. Note that the average value of δ obtained from the dynamic simulation of the detailed model was used in Table 5.2.

Table 5.2 Rotor angle from simulations compared with rotor angle from torque vs. δ curves.

MODEL	δ - T vs. δ	δ - simulated	% DIFF
detailed model	0.222	0.202	9.2
average model	0.311	0.315	-1.3

The agreement shown in Table 5.2 is quite close, and may in fact be closer since linear interpolation was used to find δ from Fig - 5.5 and Fig - 5.6. It has been shown that the currents and torques are indeed similar to those of Chapter 4. Furthermore, the rotor speed oscillations are not unexpected in light of the work presented by Russell and Pickup [9]. Therefore, it is concluded that the simulation is functioning properly.

5.5 Dynamic Simulation - Step Change in Load Torque

Model response for a step change in load torque was simulated next. A load of $1 \text{ mN}\cdot\text{m}$ was applied to the shaft of the motor after it was operating in the steady state. In order not to exceed the maximum torque limitations of the motor, the the damping coefficient was reduced to $1 \mu\text{N}\cdot\text{m}\cdot\text{sec}$. The simulation results are shown in Fig - 5.13 through Fig - 5.16

There is a huge difference in the response of the models. The detailed simulation shows that the motor will lose synchronism and the rotor speed will fall. On the other hand, the average model slows slightly, then pulls back into synchronism and operates with a new δ . The applied torque exceeded the transient stability limit for the detailed model but not the average model.

The motor should be able to meet the required load torque. In fact, a larger load was on the machine for the studies of section 5.4. It was decided to re-run the simulation with the load present at startup. After the motor reaches steady state, the load will be removed. Fig - 5.17 through Fig - 5.20 display the results for this case.

As expected, the motor ran with the applied load. The dynamics of the detailed model are quite slow, however, it is clear that synchronism is retained. The response of the average model is practically a mirror image of its response when the load was applied. Fig - 5.20 clearly shows that the machine torque decreases after the load is removed and it decays to the value needed to overcome the damping term. Notice that while in this case, both the detailed and average simulation show stable operation, the dynamics of the machine models are quite different. In particular, it is seen that the parameters of the average model exhibit approximately 13 Hz oscillations about a constant value which decay with a time constant of about 4.35 seconds. On the other hand, the parameters of the detailed model oscillate at about 1.2 Hz and have a time constant which was too large to be measured.

5.6 Explanation of Model Differences

The factor which most influences the discrepancies in results between the average and detailed dq model is the third harmonic current. Because this current is not included in the average model, larger torques are produced by the machine for a given rotor angle. Therefore, in steady state, the average model operates with larger δ than the detailed simulation; for this reason, the machine currents are not the same. It has also been demonstrated that the

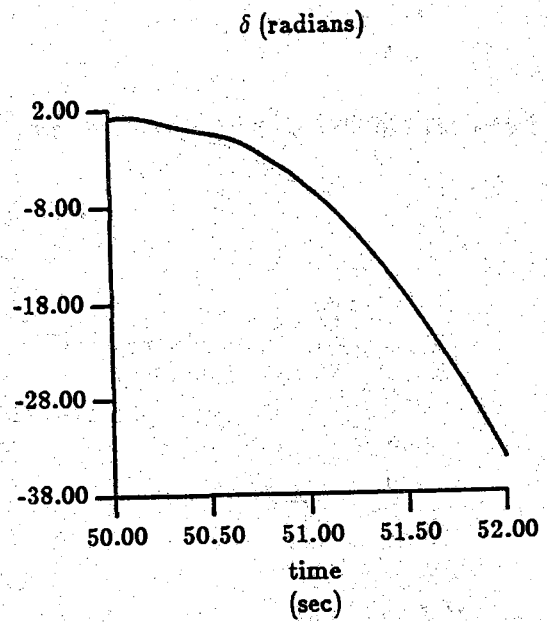
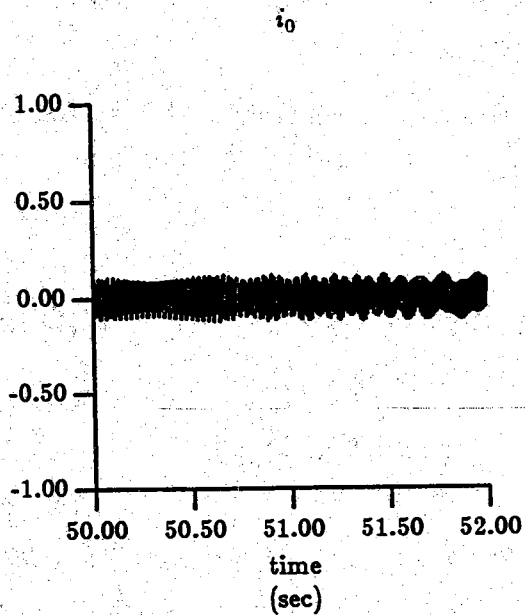
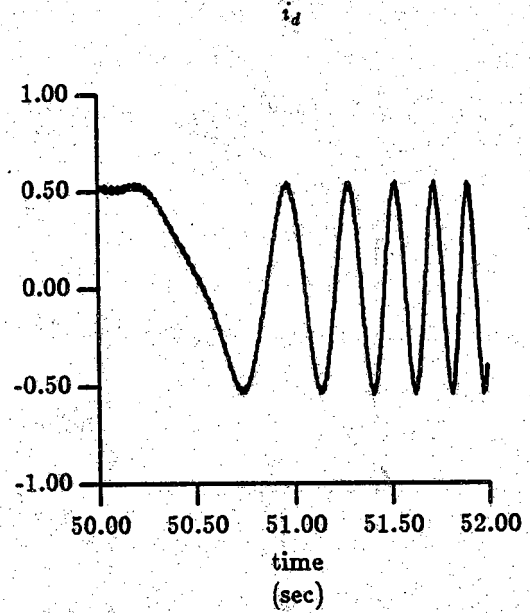
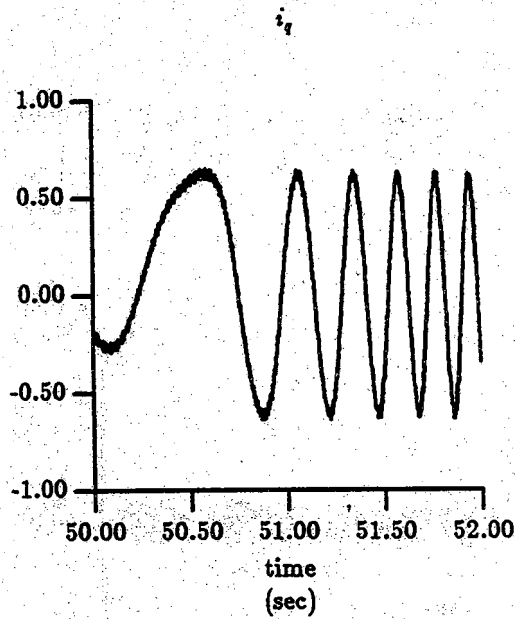


Figure 5.13 Machine currents and rotor angle vs. time (detailed model, load applied).

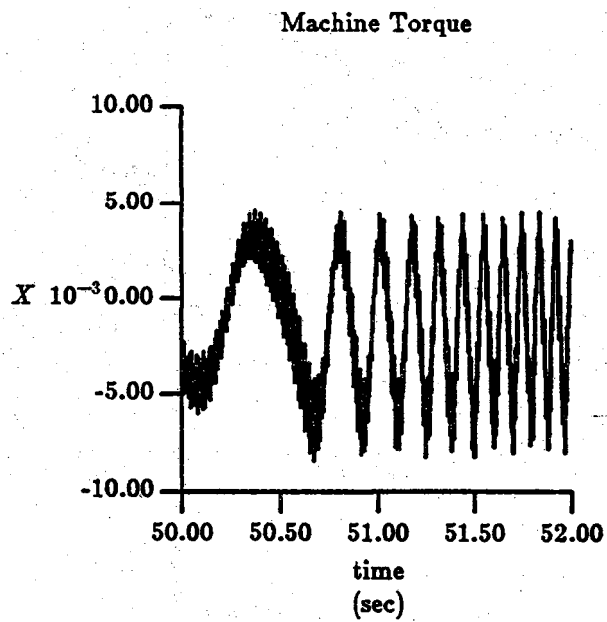
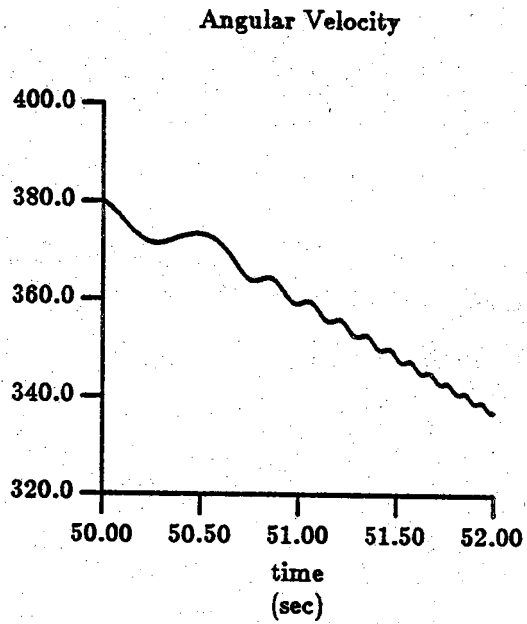


Figure 5.14 Angular velocity and machine torque vs. time (detailed model, load applied).

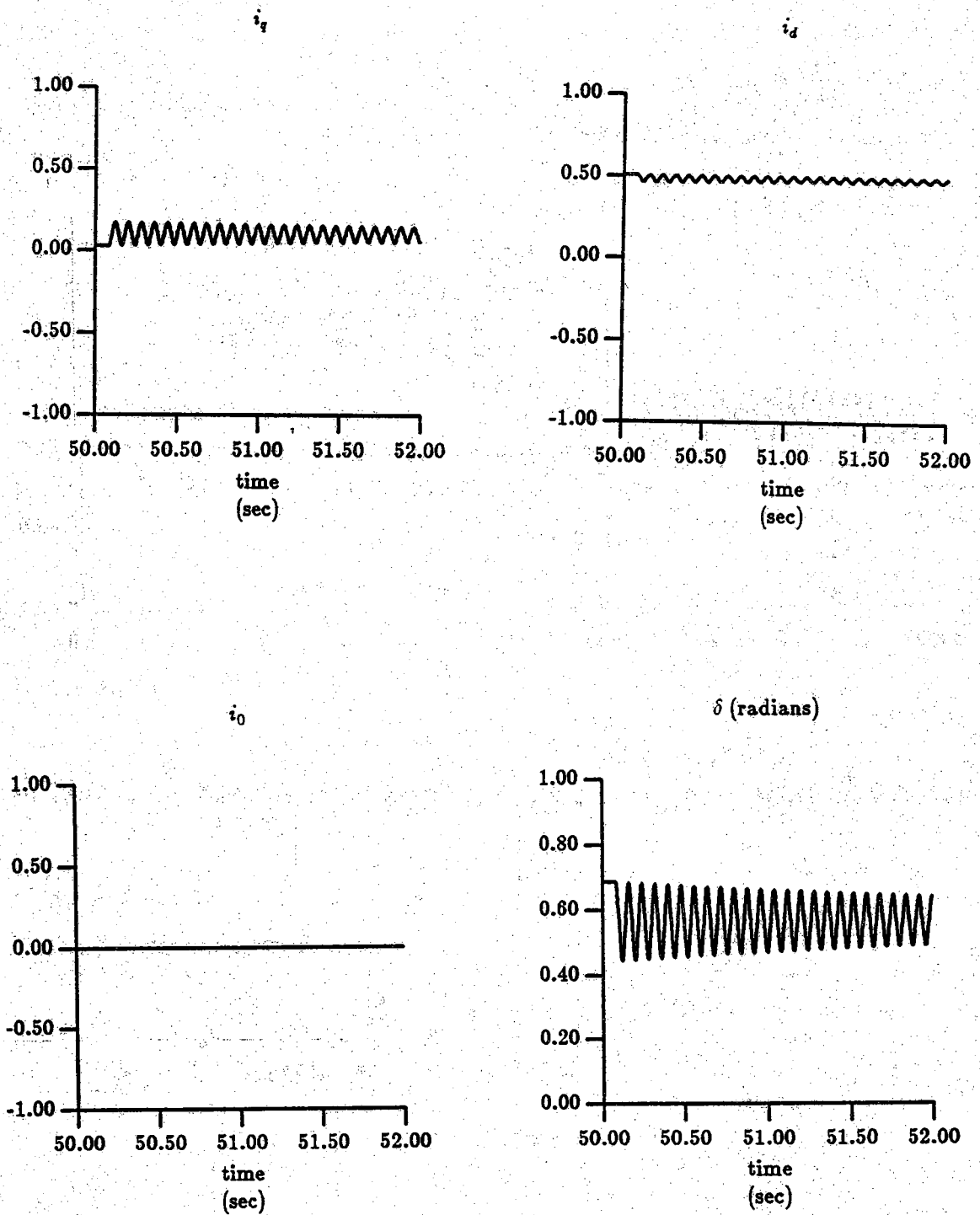


Figure 5.15 Machine currents and rotor angle vs. time (averaged model, load applied).

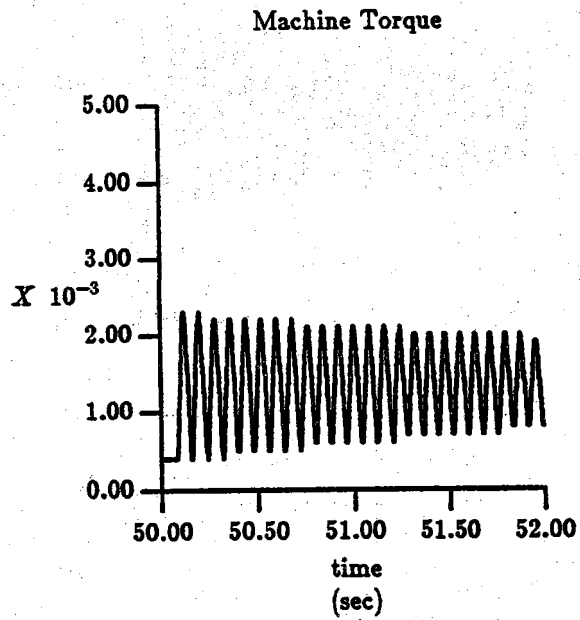
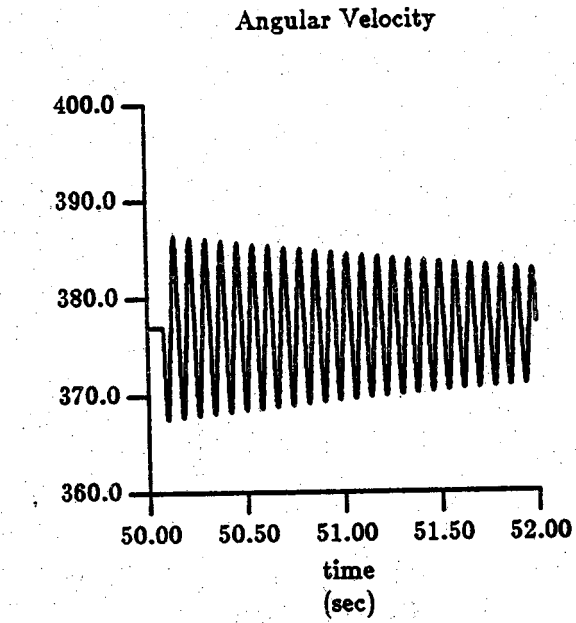


Figure 5.16 Angular velocity and machine torque vs. time (averaged model, load applied).

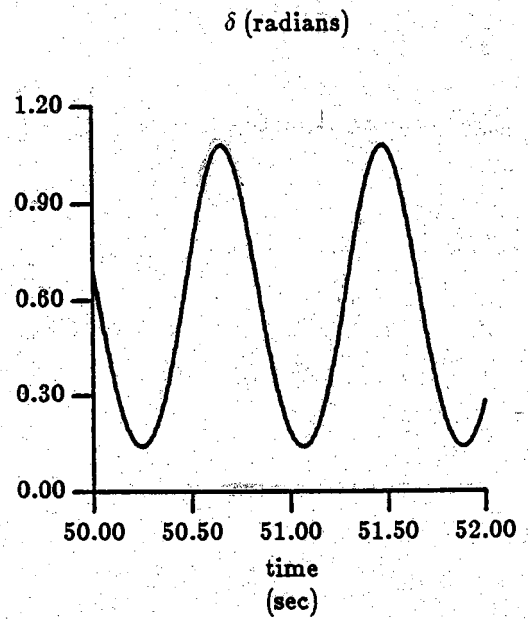
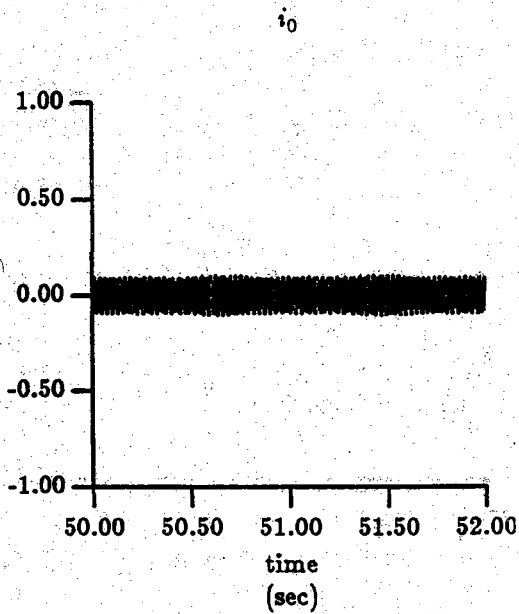
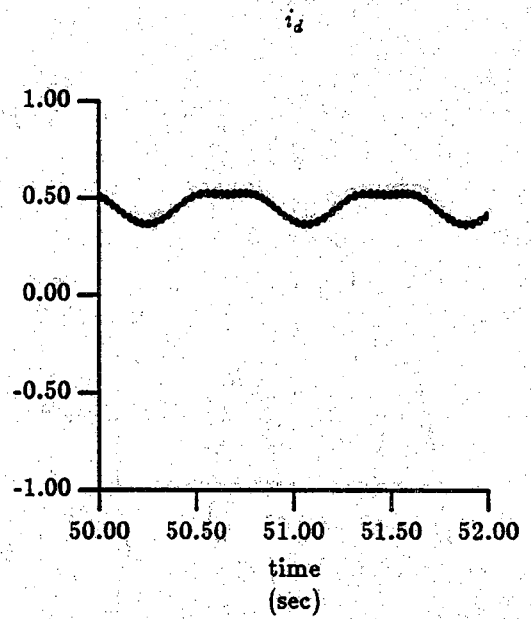
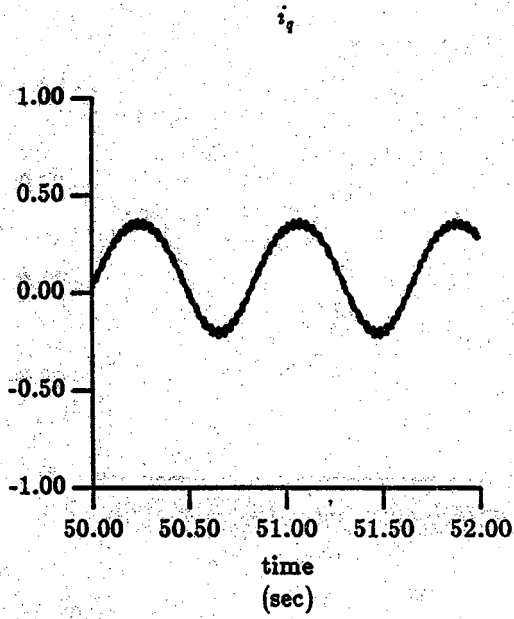


Figure 5.17 Machine currents and rotor angle vs. time (detailed model, load removed).

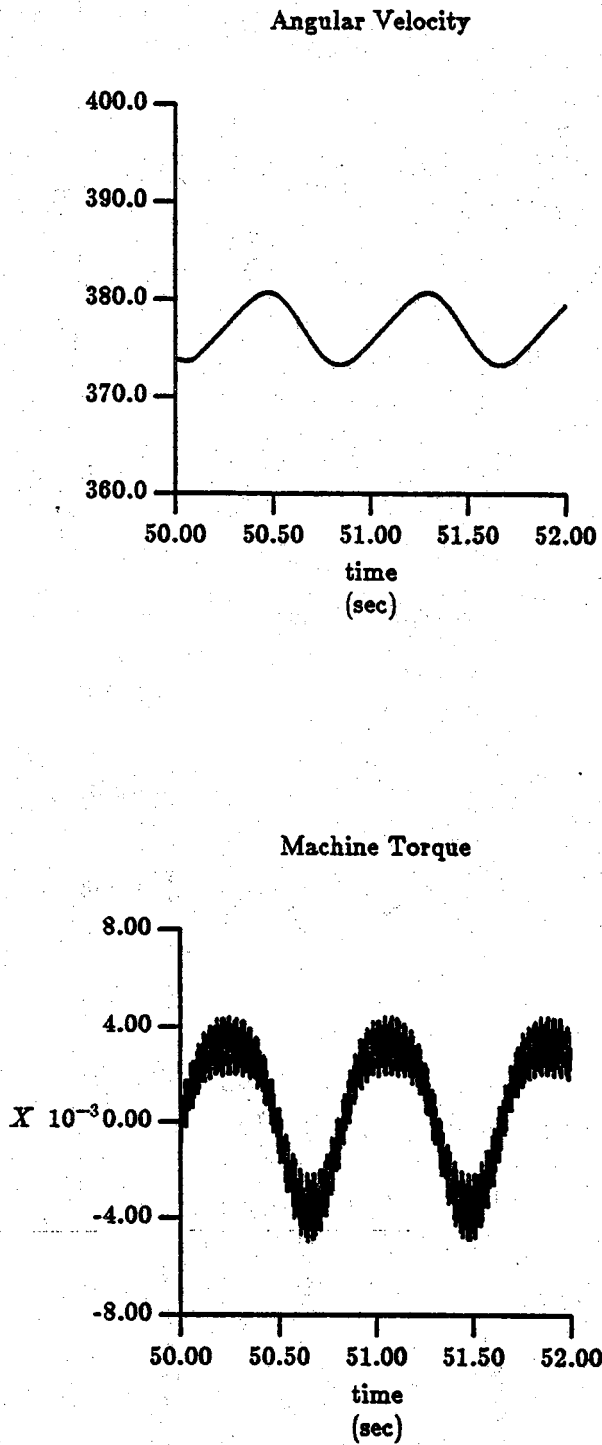


Figure 5.18 Angular velocity and machine torque vs. time (detailed model, load removed).

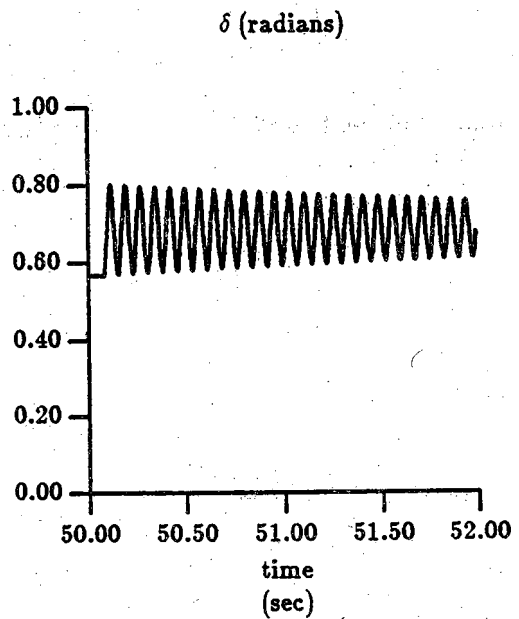
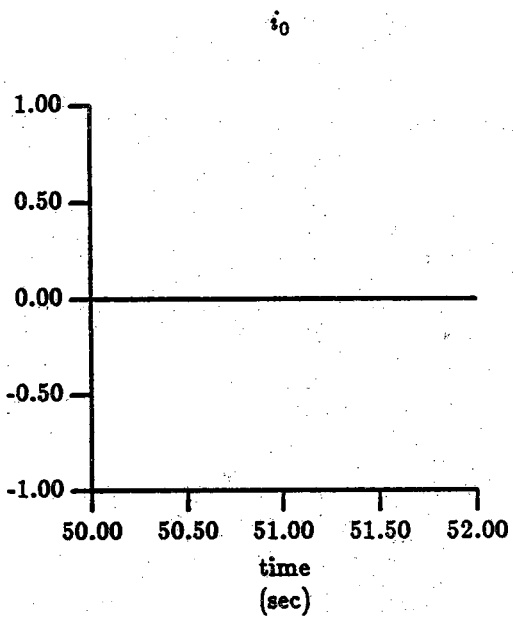
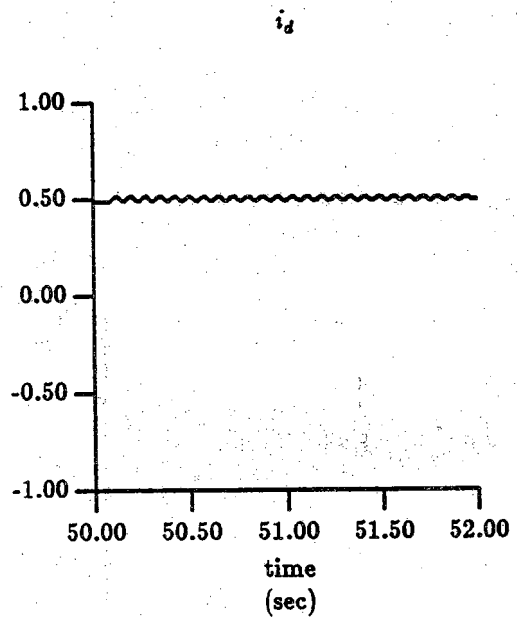
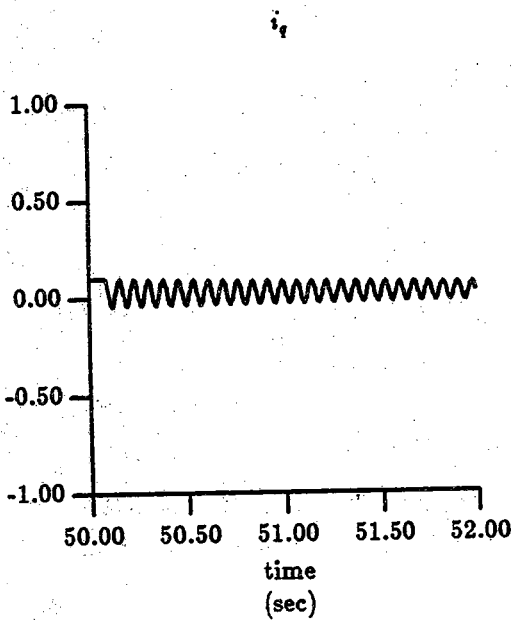


Figure 5.19 Machine currents and rotor angle vs. time (averaged model, load removed).

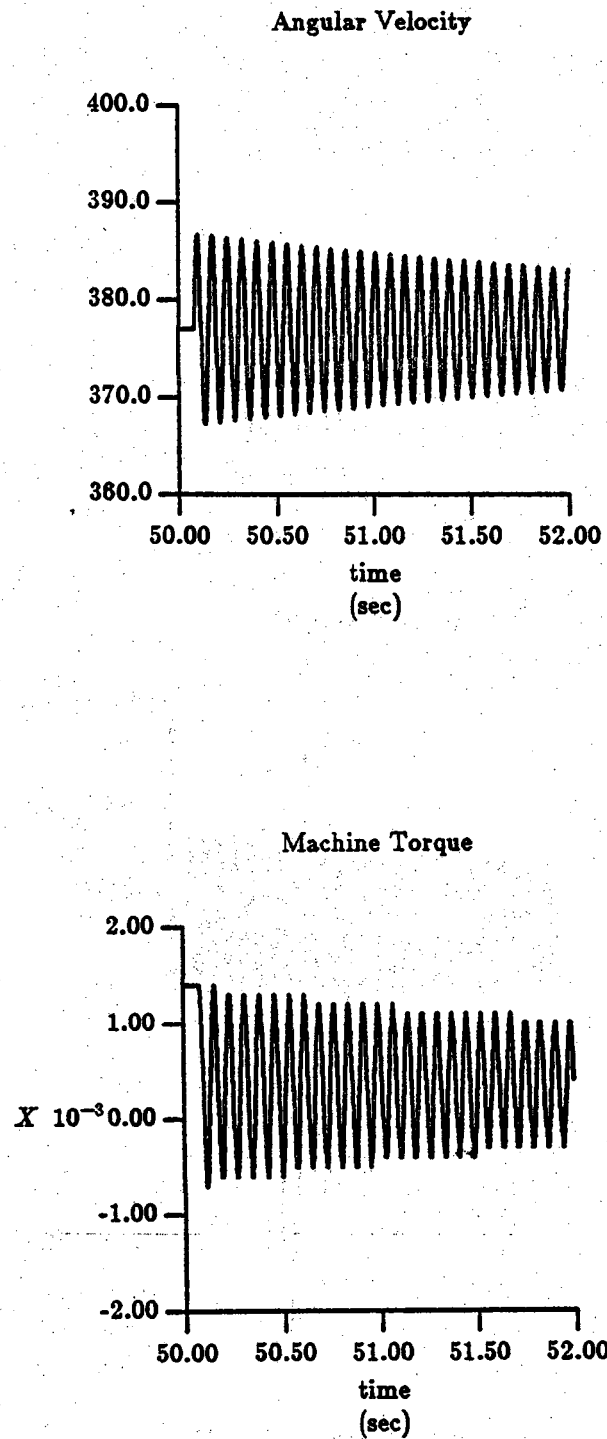


Figure 5.20 Angular velocity and machine torque vs. time (averaged model, load removed).

mechanical portion of the two models does not behave in the same manner. The average model does not show the slow oscillations which are present in the detailed model, and the dynamic response of the models after a step change in load torque is different. This is best explained by transforming the averaged flux linkage matrix back to abc variables. The flux linkage matrix is:

$$\begin{bmatrix} \lambda_a \\ \lambda_b \\ \lambda_c \end{bmatrix} = \begin{bmatrix} A - \frac{B}{3} \cos 2\theta_r & -\frac{B}{3} \cos 2(\theta_r - \frac{\pi}{3}) & -\frac{B}{3} \cos 2(\theta_r + \frac{\pi}{3}) \\ -\frac{B}{3} \cos 2(\theta_r - \frac{\pi}{3}) & A - \frac{B}{3} \cos 2(\theta_r - \frac{2\pi}{3}) & -\frac{B}{3} \cos 2(\theta_r + \pi) \\ -\frac{B}{3} \cos 2(\theta_r + \frac{\pi}{3}) & -\frac{B}{3} \cos 2(\theta_r + \pi) & A - \frac{B}{3} \cos 2(\theta_r + \frac{2\pi}{3}) \end{bmatrix} \begin{bmatrix} i_a \\ i_b \\ i_c \end{bmatrix} \quad (5.6-1)$$

This inductance matrix is of the form that would be expected for a reluctance machine with mutual coupling. Notice that the inductances *have been changed* from the values found in the original inductance matrix of Chapter 2. For this reason, it is not surprising that the two models exhibit a different transient response. In light of the discrepancies shown in this section, it is concluded that the average model *does not* adequately represent the operation of a variable reluctance stepper motor.

CHAPTER 6

SUMMARY AND CONCLUSIONS

In this thesis, a method of analysis for a variable reluctance stepper motor has been proposed and analyzed. First, the salient characteristics of stepper motors and particular applications which can benefit from these salient points were discussed. Motivation for a new analysis technique came from difficulties previous methods had in predicting such things as parametric instability, pullout torque and torque speed curves.

A brief discussion of the principles of operation of a stepper motor contributed to the development of a mathematical model which would predict the electrical and mechanical characteristics of the motor. Park's dq transformation was applied to the model in an attempt to eliminate the time varying terms present in the original machine model. The time varying terms were not eliminated by Park's transformation, so, under the assumption that the transformed currents were dc, an expression for the average flux linkages was obtained. A time-invariant, diagonal flux linkage matrix was thus obtained; this formed the basis of the proposed new model.

Digital computer simulations of the motor were developed and used to compare the results obtained from the averaged model with those from the detailed model. The average model appeared to give good results when only electrical dynamics were considered, however, simulations which included the mechanical part of the model showed certain discrepancies between the models. It appears that the averaged model is more oscillatory than the detailed model, and the response of each model to a step change in load torque is different. It is therefore recommended that great care be exercised when using the averaged model for design or analysis of systems involving a variable reluctance stepper motor.

LIST OF REFERENCES

LIST OF REFERENCES

- [1] P.C. Krause, *Analysis of Electric Machinery*. McGraw Hill, 1986.
- [2] A.E. Fitzgerald, C.D. Kingsley, Jr., S.D. Umans, *Electric Machinery*. McGraw Hill, 1983.
- [3] K. Ogata, *Modern Control Engineering*. Prentice-Hall, 1970.
- [4] R.H. Park, "Two-Reaction Theory of Synchronous Machines - Generalized Method of Analysis - Part I," *AIEE Trans.*, Vol.48, July 1929, pp. 716-727.
- [5] V.D. Hair, "Constant-Speed Stability Analysis of Variable Reluctance Step Motors," Proceedings of the 13th Annual Symposium on Incremental Motion Control Systems and Devices, University of Illinois, 1984.
- [6] P.C. Krause, O. Wasynczuk, *Electromechanical Motion Devices*. McGraw Hill, 1989.
- [7] G.T. Heydt, *Computer Analysis Methods for Power Systems*. Macmillan, 1986.
- [8] R.A. DeCarlo, *Linear Systems - A State Variable Approach with Numerical Implementation*. Prentice Hall, 1989.

- [9] A.P. Russell, I.E.D. Pickup, "High-frequency instabilities in variable-reluctance stepping motors," *Proc. of IEEE*, Vol. 125, No.9, Sept, 1978.